Dual inhibition of PDK1 and Aurora Kinase A: an effective strategy to induce differentiation and apoptosis of human glioblastoma multiforme stem cells

Simona Daniele[a#], Simona Sestito[a#], Deborah Pietrobono[a], Chiara Giacomelli[a], Grazia Chiellini[b], Danilo Di Maio[c], Luciana Marinelli[d], Ettore Novellino[d], Claudia Martini[a*], Simona Rapposelli[a*].

[a]Department of Pharmacy, University of Pisa, 56126 Pisa, Italy.

[b]Department of Pathology, University of Pisa, 56126 Pisa, Italy.

[c]Scuola Normale Superiore, Piazza dei Cavalieri 7, I-56126 Pisa, Italy.

[d]Department of Pharmacy, University of Naples Federico II, Napoli, Italy.

#These authors contributed equally to this work.

*Correspondence and requests for materials should be addressed to C.M. and S.R., Department of Pharmacy, University of Pisa, Via Bonanno 6, 56126 Pisa, Italy. E-mail addresses claudia.martini@unipi.it; simona.rapposelli@unipi.it.

Abstract

The poor prognosis of Glioblastoma Multiforme (GBM) is mainly attributed to drug resistance mechanisms and to the existence of a subpopulation of glioma stem cells (GSCs). Multi-target compounds able to both affect different deregulated pathways and the GSC subpopulation could escape tumour resistance, and most importantly, eradicate the stem cell reservoir.

In this respect, the simultaneous inhibition of Phosphoinositide-dependent kinase-1 (PDK1) and Aurora Kinase A (AurA), each one playing a pivotal role in cellular survival/migration/differentiation, could represent an innovative strategy to overcome GBM resistance and recurrence.

Herein, the cross-talk between these pathways was investigated, using the single-target reference compounds MP7 (PDK1 inhibitor) and Alisertib (AurA inhibitor). Furthermore, a new ligand, SA16, was identified for its ability to inhibit the PDK1 and the AurA pathways at once, thus proving to be a useful tool for the simultaneous inhibition of the two kinases. SA16 blocked GBM cell proliferation, reduced tumour invasiveness, and triggered cellular apoptosis. Most importantly, the AurA/PDK1 blocker showed an increased efficacy against GSCs, inducing their differentiation and apoptosis. To the best of our knowledge, this is the first report on combined targeting of PDK1 and AurA. This drug represents an attractive multi-target lead scaffold for the development of new potential treatments for GBM and GSCs.

Key words: Glioblastoma Multiforme; glioma stem cells; phosphoinositide-dependent kinase-1; Aurora Kinase A; multi-target compounds.

Introduction

Glioblastoma (GBM), a grade IV glioma, is a brain tumour displaying a high rate of recurrence and poor prognosis due to its invasive nature[1]. Current GBM therapies, including radiation followed by the chemotherapeutic agent temozolomide (TMZ), do not yield definitive effects, and the five year survival rate for GBM is less than 5% in adults[2]. GBM relapse is ascribable to the invasive nature of this tumour, as well as to its resistance to therapy.[3, 4] The incidence of GBM has been related to genetic and molecular alterations of different signalling pathways, including the epidermal growth factor receptor (EGFR) and phosphatidylinositol 3-kinase (PI3K)/Akt. In particular, the 3-Phosphoinositide-dependent kinase-1 (PDK1) inhibition has been suggested to block the oncogenic cellular processes[5, 6]. Moreover, PDK1 phosphorylates and activates Akt, thus playing a pivotal role in cell survival and tumorigenesis[6]. Overexpression of PDK1 correlates with an aggressive phenotype and poor prognosis[7]. Therefore, drugs targeting the PDK1/Akt pathway have emerged as one of the potential treatments for GBM[8-10]. However, specific target drugs, including those against PDK1, did not show a significant clinical efficacy[11], and preclinical studies on PDK1 inhibitors have been hampered by the lack of peculiar proof-of-concept molecules[5,12-14]. In fact, canonical drug resistance processes include an increased expression of efflux pumps, drug target alterations, over-activation of pro-survival pathways[15], and most important, clonal heterogeneity [16, 17].

Recently, GBM recurrence and resistance to therapies have also been related to the presence of GBM stem-like cells (GSCs), a sub-population of multipotent tumour-initiating cells displaying stem cell-like characteristics[18, 19]. Aggressiveness and unresponsiveness of gliomas have been correlated with the number of GSCs[3], and long-term temozolomide (TMZ) treatment has been shown to favour the emergence of drug-resistant GBM cells[20], indicating that a stem cell-oriented therapy is needed to prevent GBM recurrence and to improve the outcome of treatments.

Eradication of the GSC reservoir, by blockade of key pathways involved in stem cell maintenance, has been found to effectively reduce their tumorigenic potential[21, 22]. Among these pathways, the Aurora kinase A (AurA) has emerged as an effective target. AurA is a serine–threonine kinase that plays a pivotal role in cellular proliferation and differentiation of several tumours, including GBM[23, 24]. In particular, AurA is expressed in gliomas and is associated with patient survival, thus representing a potential therapeutic target for GBM[25]. More important, blocking the AurA pathway resulted in inhibition of GSC colony formation and potentiation of the common GBM chemotherapeutics[23]. On the basis of these considerations, a multi-target approach[16] that is able to impact multiple deregulated and escape pathways, and deplete the GSC reservoir, may offer the most promising strategy for the treatment of GBM and minimize drug resistance. Among these

approaches, the simultaneous disruption of PDK1 and AurA, each one playing a pivotal role in the cellular survival/migration/differentiation, could represent an innovative strategy to overcome GBM resistance and recurrence. In this respect, a few compounds, classified as PDK1 inhibitors, have been shown to also affect AurA activity. For instance, OSU-03012, a PDK1 inhibitor, was found to affect multiple cellular targets, including the AurA one, in neuroblastoma and other cancer cells[26], thus supporting the aforementioned mechanistic rationale (Fig. 1).

Herein, the molecular mechanisms at the basis of a simultaneous PDK1/AurA inhibition were explored in different GBM cell lines, as well as in a GBM-derived stem-like culture. As a first step, the standard PDK1 inhibitor, MP7[12], and the AurA blocker Alisertib (MLN8237)[23] were used as reference compounds to investigate the functional crosstalk between the two pathways in GBM. Furthermore, starting from previously synthesized PDK1 inhibitors, namely OXID-pyridonyl hybrids[9, 10], we identified SA16 as a new ligand able to inhibit both the PDK1 and the AurA pathways at once and thus useful in establishing the preclinical proof of mechanism for the simultaneous inhibition of these two pathways (Fig. 1). The new identified compound decreased GBM cell proliferation, triggered cellular apoptosis and reduced cell invasiveness. Moreover, this novel AurA/PDK1 blocker showed a marked efficacy on GSCs by inducing differentiation and apoptosis.

To the best of our knowledge, this is the first study reporting a combinatorial treatment strategy based on the simultaneous inhibition of PDK1 and AurA. Furthermore, we identified an innovative PDK1/AurA dual-target molecule which could represent an attractive lead scaffold for the design and synthesis of new multi-target treatments for GBM and, most importantly, for GSCs.

Results and Discussion

The combined inhibition of PDK1 and AurA affects GBM cell proliferation.

In order to study the combined effects of PDK1 and AurA inhibition, the U87MG cells were chosen as representative GBM cell line, since they are characterised by: i) the lack of the tumour suppressor phosphatase and tensin homologue (PTEN), a negative regulator of the Akt pathway[27, 28], and ii) the expression of a functional AurA[25].

First, we assessed the effects on adherent U87MG cell proliferation following combined inhibition of the two kinases. The experiments were performed in the presence of the PDK1 inhibitor MP7, alone or in combination with the AurA inhibitor, Alisertib. These reference compounds were used starting from a concentration corresponding to the IC_{50} value on the target kinases[29, 30].

Following 72 h treatment, MP7 alone did not show a significant inhibition of GBM proliferation (Fig. 2A), consistent with previous reports[12]. Indeed, MP7 has been shown to have only minimal effects on monolayer cell growth in several cancer cell lines, with IC_{50} values in the micromolar range[12], suggesting that PDK1 activity is not rate-limiting for cell proliferation but rather in cell migration/invasion[12] .

Alisertib alone slightly reduced U87MG cell proliferation (Fig. 2A), showing a significant effect of inhibition at 1.5 μM. Consistent with our data, an anti-proliferative effect was reported recently by Lehman and co-workers in monolayer GBM cell lines, including U87MG cells[25], with IC_{50}'s ranging from 60 to 225 nM[25]. An increased blockade of GBM proliferation was noticed when the cells were challenged simultaneously with MP7 and Alisertib: the combined treatment with the two compounds showed synergic/additive anti-proliferative effects at all the concentrations tested when compared to single-treated cells (Fig. 2A), with a maximal percentage of inhibition of 58.5 ± 4.9 %. Further experiments will clarify if MP7 and Alisertib produce a synergic or rather an additive effect. Cell counting confirmed that MP7 and Alisertib administered individually slightly affected U87MG cell viability at the highest concentration (Supplementary Fig. 1). When U87MG cells were probed simultaneously with the two inhibitors, a significant amplification in the decrease of live cells was observed with respect to single-treated cells (Supplementary Fig. 1); at the highest concentrations, MP7 and Alisertib significantly enhanced the number of dead cells as well (Supplementary Fig. 1). These data demonstrate that the reduction of GBM proliferation shown by the MTS assays can be attributed, at least in part, to a decrease of U87MG live cells.

Taking into account the heterogeneity of cancer cell lines, and with the aim of further consolidating our data, additional proliferation experiments were performed using different GBM cell lines (i.e. ANGM-CSS and U343MG cells). Indeed, these cells present slight differences in motility and

invasiveness, and different expression of proteins involved in tumour progression, angiogenesis and apoptosis [31]. The AuraA inhibitor Alisertib lead to a significant reduction of MTS measurements starting from 150 nM in U343MG and ANGM-CSS cells (Supplementary Fig. 2A and B). Similarly to what observed in U87MG cells, MP7 did not cause a significant decrease of U343MG or ANGM-CSS proliferation (Supplementary Fig. 2A and B). In contrast, the combination of MP7 and Alisertib showed greater effects with respect to single- treated cells (Supplementary Fig. 2A and B). Thus, even with the great heterogeneity of GBM, the combined use of MP7 and Alisertib showed promising effects in the three tested cell lines, suggesting that the simultaneous inhibition of PDK1 and AurA can be a useful strategy to inhibit GBM cell proliferation.

The combined inhibition of PDK1 and AurA affects GSC proliferation and induces their differentiation.

GSCs are the self-renewing compartment of cancers, thus representing an essential target of innovative therapies. Both PDK1 and AurA have been demonstrated to play an important role in GSC survival/differentiation: recent evidences suggest that blocking PDK1 is essential to induce GSC apoptosis[4]; similarly, the inhibition of AurA has been shown to result in antiproliferative effects towards GSCs[23]. Therefore, in order to shed light on the effects elicited by the combined inhibition of the two kinases, Alisertib and MP7 were probed on GSCs isolated from U87MG cells.

The formation of GSC neurospheres *in vitro* was obtained using a specific neural stem-cell (NSC) medium, as previously described[32]. Consistent with literature data[33], neurospheres were confirmed to contain a higher portion of GSCs than the monolayers cells (Supplementary Fig. 3A). GSCs obtained from U87MG cells showed significantly more CD133/Nestin+ cells and a smaller percentage of GFAP+ cells than whole U87MG cells, as shown by real time PCR analysis (Supplementary Fig. 3B).

To verify the methodological reliability of the assay, the colony-forming ability of the neurospheres and their chemoresistance, which are a key feature of GSCs, were evaluated. As demonstrated in Supplementary Figure 4, the sphere formation ability was significantly enhanced in GSCs with respect to whole U87MG population (47.5% GSC, 9.9% U87MG, $p<0.001$). These data indicate that GSCs are highly clonogenic and possess self-renewal ability, and that the U87MG adherent cells retain a slow stem potential.

Challenging cells with the alkylating agent TMZ for 72 h showed a reduction in cell proliferation of 50.0 ± 2.7 and 15.0 ± 3.5 in U87MG and in GSCs, respectively (Supplementary Fig. 5, $p<0.001$). These data demonstrate that stem-like GBM cells exhibited a higher resistance to TMZ with respect

to U87MG adherent cells, and overall confirm the methodological consistency of neurosphere isolation.

Then, the effects of MP7 and Alisertib administered as single agents and in a combinatorial fashion, were assessed in GSCs. Consistent with the data obtained in U87MG cells, MP7 alone showed slight effects on tumorsphere proliferation (Fig. 2B). It can be speculated that PDK1 inhibition is related to GSC formation rather than to their proliferation. Indeed, PDK1 has been shown to deplete the cancer stem cell (CSC) population in highly invasive breast cancer cells by decreasing tumorspheres formation but not their proliferation[34]. In contrast, Alisertib induced anti-proliferative effects on GSCs, in a concentration-dependent manner (Fig. 2B), thus demonstrating that AurA inhibition shows a great efficacy in neurosphere cells. Indeed, GSCs have been shown to be highly disposed to aberrant cell division and polyploidization, with a pronounced change in the dynamic of mitotic centrosome maturations, and thus are strongly dependent on AurA[35]. In a recent work, it has been reported that moderate AurA inhibition is linked to spindle defects, polyploidization and a dramatic increase in cellular senescence[35]. Consistent with these findings, Alisertib treatment has been shown to inhibit the colony-formation ability of GSCs isolated from patients with IC_{50} in the low nanomolar range[23].

The combination of the two compounds decreased GSC proliferation, in a concentration-dependent manner, with percentages of inhibition significantly higher with respect to those obtained in single-treated GSCs (Fig. 2B).

Similar results were obtained in MTS experiments using neurospheres isolated from U343MG (Supplementary Fig. 6A) or ANGM-CSS (Supplementary Fig. 6B).

Cell counting of U87MG-derived GSCs confirmed that Alisertib and, to a minor extent, MP7 were able to decrease the number of viable cells (Supplementary Fig. 7). When combined together, GSC viability was further reduced with respect to single-treated cells (Supplementary Fig. 7). As observed in U87MG cells, when used at the highest concentrations (i.e. 1.5 μM Alisertib and 2.5 μM MP7), a significant enhancement in the number of dead cells was evidenced (Supplementary Fig. 7).

Globally, these preliminary results suggest that the combined use of 1.5 μM Alisertib and 2.5 μM MP7 efficaciously affect proliferation/viability of the GSC subpopulation.

Subsequently, the effects of MP7, Alisertib and their combination on GSC morphology were evaluated. To this purpose, 1.5 μM Alisertib/2.5 μM MP7 was chosen as the representative combination of the two inhibitors. The cells were incubated with 2.5 μM MP7, alone or in combination with 1.5 μM Alisertib for seven days. The two compounds, when administered

individually, led to a reduction in the area occupied by the neurospheres (Fig. 3A and B); these effects were particularly evident in cells treated with Alisertib. Moreover, after treatment with Alisertib, GSCs also showed a modest but significant outgrowth of cellular processes (Fig. 3A and C), implying that AurA blockage can induce GSC differentiation. Consistent with this hypothesis, the AurA inhibitor AKI603 has been shown to promote cell differentiation of chronic myeloid leukaemia cells[36]. When MP7 and Alisertib were given in combination, a synergic/additive effect on the reduction of neurospheres'area was evidenced (Fig. 3A-B), thus suggesting that the combined inhibition of PDK1 and AurA could be a useful strategy to inhibit GSC proliferation. Further experiments will be needed to clarify the role of each kinase in survival and differentiation of tumour stem-like cells and the mechanism responsible for the enhanced response elicited by the combined inhibition of both pathways.

Molecular Modeling

Aiming at identify new scaffolds for the synthesis of novel PDK1 inhibitors, we have designed a new class of OXID-pyridonyl compounds[9, 10]. Among these hybrids we developed SA16 (Fig. 1B), which was identified as a putative ligand with the ability to inhibit both the PDK1 and AurA kinases at once. SA16 was originally designed as a PDK1 inhibitor by combining two pharmacophoric moieties known to bind the ATP binding site and the DFG-out pocket of PDK1, through a phenylglycine linker. Since many published data report that several PDK1 inhibitors with a high grade of hydrophobicity (i.e. OSU-03012 and BX795) also show affinity for AurA, we decided to investigate the activity of SA16 against other kinases. Consequently, SA16 was subjected to FRET-based Z′-Lyte assay (Invitrogen) against 56 kinases at 500 nM concentration (see Supporting information Table 1). We thus found that SA16 possessed a significant inhibition potency against both PDK1[10] (IC_{50} = 416 nM) and Aur A (IC_{50} = 35 nM), suggesting that this compound could be studied as a prototype of dual PDK1/Aur A inhibitor.

To gain insights into the mechanism of dual PDK1/AurA inhibition and to elucidate the binding mode of SA16, we carried out molecular docking calculations. In a previous computational study we showed that OXID-pyridonyl hybrid compounds most likely bind to the DFG-out conformation of PDK1[10]. The docking analysis presented here shows that SA16 inserts its 1-[3,4-difluorobenzyl]-pyrid-2-one moiety into a pocket, characteristic of the DFG-out conformation, carved by Met-134, Leu-137, Phe-142, Val-143, Leu-196, Leu-201, His-203, Ile-221, Asp-223 and Ala-227 (Fig. 4A). Within such pocket, several CH-π interactions are established by the 3,4-difluorobenzene ring with Leu-137, Leu-196 and Asp-223 and by the 2-pyridone ring and Val-123. Additionally, the amidic

carbonyl and the carbonyl group in the 2-pyridone ring engage in hydrogen bonds with the side chain of Lys-111 and the Asp-223 backbone NH, respectively. As previously observed for analogue compounds[10], SA16 positions itself in a way that, while still allowing to form CH-π interactions with Val-143, Leu-212 and Thr-222, prevents it from establishing hydrogen bonds with the hinge region residues (i.e. Ser-160 and Ala-162), likely to minimize steric clashes between the phenyl ring on the methylene of the linker and Ser-94 and Val-96. Specifically, a 100ns-long MD simulation performed on an analogue compound confirmed this finding, suggesting that it is not an artifact of the rigid-docking procedure. However, the formation of a salt bridge between the imidazole ring, which is likely protonated owing to a favorable electrostatic environment, and Glu-166 could at least partially compensate for the loss of these interactions.

Unlike the binding to PDK1 described above, the AurA conformation that binds to SA16 is not known, and the fact that the pocket characteristic of the DFG-out conformation seems to be narrower in AurA than in PDK1 casts some doubts on the likelihood that SA16 binds the same way to both enzymes. Indeed, not only the αC helix is more structured and closer to the N-terminal lobe in AurA than in PDK1, but some of the DFG-out pocket lining residues in AurA (Gln-185, Leu-194 Arg-225) are relatively bulkier, as compared to those found at the corresponding positions in PDK1 (Met-134, Val-143 and His-203). Overall these two factors contribute to make the DFG-out pocket of AurA narrower, likely hampering an efficient accommodation of the 1-[3,4-difluorobenzyl]-pyrid-2-one moiety. A further issue in the selection of a suitable receptor structure for docking calculations is the high conformational variability of AurA, which makes this protein a challenging system to treat via molecular modeling approaches. Indeed, in addition to the inherent flexibility of the glycine-rich loop common to most kinases, it is known that inhibitors can induce structural changes in AurA leading not exclusively to the canonical "in"/"out" states, but also to a number of other distinct conformations of the DFG motif[37-43]. It was thus not practical to pick out *a-priori* the most suitable receptor conformation. A more exhaustive approach had therefore to be adopted to identify the binding mode of SA16 in AurA. Accordingly, seven AurA structures in complex with different ligands, representative of just as many different conformations, were selected for docking calculations (see Supporting information for details on the selection criteria, Supplementary Table 2).

Docking calculations were able to assign unambiguously a clear binding mode for SA16 only in one of the selected structures (PDB code: 4UZH). In this case, results converged to mostly one solution, depicted in Figure 4C, regardless of the protonation state considered for the imidazole ring. Specifically, the ((Z)-3-((1H-imidazol-4-yl) methylene)indolin-2-one) moiety inserts within the

hinge region of AurA establishing CH-π interactions with Leu-139, Val-147, Ala-160, Leu-263, together with hydrophobic contacts with Leu-194, Leu-210 and Tyr-212. Moreover, the carbonyl group of the indolin-2-one ring and the N_δ-H of the imidazole engage in hydrogen bonds with Ala-213 NH and CO backbone groups, respectively. Most of the docking poses feature a charged or N_δ-protonated imidazole: however, we believe that the latter is the more likely protonation state, owing to its close proximity to Arg-220 and Arg-137 in the binding mode predicted by docking. Hydrogen bonds are also formed between the carbonyl oxygen of the amidic groups linked to both the indolin-2-one and the 2-pyridone rings and Lys-162. The 3,4-difluorobenzene ring is favorably hosted in a quite large hydrophobic pocket, where the 3,4-difluorobenzene ring makes several CH-π, CH-F and other hydrophobic interactions with Phe-144, Lys-162, Leu-164, Leu-169, Val-174, Gln-177, Leu-178, Leu-208, Phe-275.

In conclusion, we believe that the binding mode predicted by the docking for SA16 to AurA could reasonably justify the low nanomolar activity displayed by the ligand. However, we cannot rule out that some large structural rearrangements specifically triggered by SA16, may take place, potentially leading to an unpredictable different conformation of AurA. An X-ray crystallographic structure of the AurA-SA16 complex will ultimately have to be solved before plausibly discarding this possibility.

The dual-target compound blocks GBM proliferation, but lacks toxicity in normal cells.

First, the effects of SA16 on U87MG cell growth/survival were assessed. Whereas the compound slightly affected GBM cell proliferation after 24 h of incubation (Fig. 4C), challenging cells for 72h with SA16 significantly decreased U87MG cell proliferation. These effects occurred in a concentration-dependent manner, with a maximal percentage of inhibition of 49.4 ± 2.0 % (Fig. 4D), comparable to that obtained in the simultaneous presence of Alisertib and MP7 (58.5 ± 4.9%).

As depicted in Supplementary Figure 8, SA16 significantly reduced the number of U87MG viable cells, and enhanced the number of dead cells (Supplementary Fig. 8), thus suggesting that the decrease of MTS measurements is associated with a reduction of cell viability.

Comparable effects were obtained in ANGM-CSS cells, where the dual PDK1 inhibitor decreased GBM cell proliferation after 72 h of incubation, with a maximal percentage of inhibition of 54.9 ± 4.5 % (Supplementary Fig. 9). Globally, these results demonstrate the great efficacy of the new compound in blocking proliferation/viability of different GBM cells.

To investigate the preliminary toxicity profile of SA16, both human mesenchymal stem cells (MSCs) and human lymphocytes were used as normal non-cancer cells. Challenging MSCs with

SA16 (1-100 μM) for 72 h did not significantly affect cell proliferation (Fig. 4E). Similar results were obtained in human lymphocytes (Fig. 4F), thus suggesting that SA16 mechanism of action is directed preferentially toward tumour cells.

Consistent with these data, Alisertib has been demonstrated to lack toxicity toward normal human astrocytes[23]. Similarly, PDK1 inhibitors have been extensively developed as anticancer drugs because of their low toxicity in normal cells[44]. For example, an allosteric inhibitor designed to impair PDK1 plasma membrane localisation has been shown to lack toxic effects in zebrafish embryos[45]. Thus, the dual inhibition of PDK1 and AurA kinases can represent a useful and non-toxic therapeutic strategy in cancer.

The dual-target compound induces GBM apoptosis and inhibit cell migration.

The effect on GBM proliferation/viability was accompanied by cellular apoptosis. Indeed, challenging U87MG cells with SA16 for 72 h caused a significant induction of early and late apoptosis, as demonstrated by phosphatidylserine externalisation in the absence (early apoptosis), or in the presence of 7-amino-actinomysin binding to DNA (late apoptosis/death) (Fig. 5A and B).

These data are consistent with the apoptotic effects elicited by the AurA blocker VX-680[46]. In the same paper, the authors found a correlation between cell sensitivity to AurA inhibitor and the phosphorylation status of Akt, suggesting a cooperation between AurA and Akt pathways[46].

Several data demonstrate a pivotal role for PDK1 in the regulation of cell migration[7]. Indeed, through the activation of multiple downstream effectors, this kinase represents a primary hub coordinating signals from extracellular cues to the cytoskeletal machinery, the terminal executor of cell movement[7]. On this basis, a scratch wound assay was performed following U87MG cell treatment with SA16 for 72 h. Representative images of control and treated U87MG cells are depicted in Figure 5C. Quantitative analysis of the gap area showed that SA16 significantly inhibited cell migration, both after 6 h and 24 h from the scratch (Fig. 5D). Globally, these results suggest that the new compound can efficaciously block U87MG cell migration, consistent with the data reported for MP7[12].

We speculate that the effects elicited by SA16 on tumour migration can be mainly ascribed to the PDK1 inhibition, because the overexpression of this kinase has been shown to raise tumour invasiveness[47, 48] and promote tumour growth in immunocompromised mice[49].

The dual-target compound inhibits GSC formation and viability

The effects of the new dual ligand were then assessed on the GSC subpopulation. SA16 induced a concentration-dependent inhibition of GSC proliferation, starting after four days of cell incubation (Fig. 6A and B). Following a seven-day treatment, the PDK1-AurA inhibitor yielded an IC_{50} value of 8.33 ± 0.78 nM and a maximal percentage of inhibition of 80.0 ± 2.0 % (Fig. 6B). Notably, the maximal effects of the co-treatment protocol Alisertib/MP7 (59.9 ± 2.9 %) were lower with respect to those obtained with the dual target compound SA16.

Similar effects were noticed in GSC isolated from U343MG and ANGM-CSS cells (Supplementary Fig. 10A and B); indeed, SA16 displayed IC_{50} values of 49.7 ± 3.9 nM and 44.0 ± 3.6, and maximal percentages of inhibition of 81.4 ± 1.7 % and 77.0 ± 1.8 % in U343MG-GSCs and ANGM-CSS-GSCs, respectively. These data demonstrate that the new compound can inhibit the stem-like population of GBM cells with great efficacy. Although a direct comparison between GSC and monolayer GBM cells is not possible, a preferential action of the compound toward neurospheres can be speculated. Indeed, CSCs have been shown to display extensive multiple kinase activation with respect to monolayer cells[50], and to express higher AurA levels [51], implying that CSCs are intrinsically more sensitive to AurA or PDK1 inhibition than monolayer cultures. Consistent with this hypothesis, the AurA inhibition has been demonstrated to elicit higher antiproliferative effects to neurosphere cells than to standard monolayer GBM cells[23].

The SA16-mediated reduction of GSC proliferation was associated to apoptosis/death, as demonstrated by the significant induction of phosphatidylserine externalization in the presence of 7-AAD binding to DNA (Fig. 6C and D). Globally, these results suggest that the dual target ligand is able to arrest GSC proliferation and induce their apoptosis. These effects can be attributed to both PDK1 or AurA block: indeed, a potent PDK1inhibitor has been demonstrated to reduce proliferation and to induce apoptosis of acute myeloid leukemia cells[52], while Alisertib was found to exert growth inhibitory effects and trigger apoptosis/autophagy in a leukemia cell line[53].

Furthermore, the ability of SA16 to affect GSC self-renewal was examined. To this purpose, GSC cells were dissected and a soft-agar assay was performed. The effect of a sub-toxic dose of SA16 (1 nM) was evaluated after 21 days of treatment (Fig. 6E-G). The results showed that the compound did not affect the total sphere number (Fig. 6E and G); conversely, the diameter of the newly formed spheres was significantly reduced in the presence of SA16 (Fig. 6E and F). These results suggest that SA16 has the ability to decrease the stem cell self-renewal ability of the GSCs. This effect can be ascribed to both PDK1 and AurA block. Indeed, Alisertib has been shown to potently inhibit the

self-renewal ability of GSCs[23]; similarly, PDK1 has been shown to deplete the CSC population in highly invasive breast cancer cells by decreasing tumorspheres formation[34].

The combined inhibition of PDK1 and AurA affects GSC morphology and stemness.

The effects of SA16 on GSC morphology were evaluated by quantifying the area occupied by the cells in culture plates, as well as the outgrowth of cellular processes. When the cells were incubated with SA16 for seven days at different concentrations (1μM or 10μM), an almost complete reduction in the area occupied by the neurospheres was noticed (Fig. 7A and B), and the cells showed prominent outgrowth of processes (Fig. 7A and C).

Real time PCR experiments (Fig. 7D) showed that the compound induced a significant transcription of the glial marker GFAP and of neuronal marker MAP2, thus suggesting that SA16 induced stem cell differentiation toward a neuronal and glial phenotype. These data were confirmed at the protein level by Western blotting (Fig. 8A and B), which showed a significant decrease of the stem cell marker Nestin, accompanied by a significant increase of GFAP protein levels.

We then verified if adherent GBM cells could lose their stemness potential after drug treatment. To this purpose, stem cell markers were analysed in U87MG cells treated with SA16 for 72 h. As depicted in Figure 8C, the dual compound significantly reduced the mRNA transcription levels of the stemness markers CD133 and Nestin in the remaining adherent cells with respect to the initial cell population.

Globally, these data demonstrate that PDK1-AurA inhibition is able to reduce GBM stemness potential. In agreement with our results, Alisertib was found to induce cellular differentiation in surviving GBM cells after its cytotoxic effect[25], allowing the authors to hypothesize that this differentiating effect could be ascribed to an AurA inhibition-mediated decreased c-Myc and/or NFκB signalling. Indeed, c-Myc induces Nestin expression and the undifferentiated glioblastoma tumor stem cell phenotype[54], while blockade of NFκB signalling cause senescence of differentiating glioblastoma cells[55].

Conclusions

The Akt/PDK1 and AurA pathways play a pivotal role in GBM cellular survival/migration and in the self-renewal of the glioma stem cell component, and thus could represent an innovative strategy to overcome GBM resistance and recurrence.

For the first time, the combined inhibition of the two kinases was investigated in GBM cells and in

the GSC subpopulation, using the reference compounds MP7 and Alisertib. Furthermore, SA16 was identified as a new ligand able to simultaneously inhibit both PDK1 and AurA kinases. This novel OXID-pyridonyl derivative was demonstrated to block GBM cell proliferation, reduce tumour invasiveness, and to trigger cellular apoptosis. Even more remarkable was the ability of the new AurA/PDK1 blocker to control GSCs by inducing their differentiation and apoptosis.

To the best of our knowledge, this is the first study of a combinatorial treatment strategy that simultaneously inhibits both PDK1 and AurA pathways. Finally, the innovative PDK1/AurA dual-target molecule we identified, SA16, provides a very promising multi-target approach to the treatment of GBM, with the added ability to deplete GSC population, and thus improve the prognosis of the disease.

Additional experiments will be performed to explore in more detail the intracellular proteins involved in AuroraA/PDK1 crosstalk. AurA has been demonstrated to activate mTOR/Akt/PDK1 pathway during cell transformation[46], and a more malignant phenotype is observed in AurA cells containing a higher activation of mTOR/Akt/PDK1 signals, thus suggesting a strong link between these signalling pathways.

Methods

Chemistry. The synthetic Scheme followed for the preparation of SA16 is reported in Supplementary Section (Supplementary Scheme. 1). The experimental procedures to obtain the final product have been previously reported[10]. Briefly, the N-BOC-phenylalanine was condensed with the 5-amino-2-oxo-indole, which was successively deprotected and submitted to the reaction with the appropriate carboxylic acid in the presence of TBTU and DIPEA. Consequently, the Knoevenagel reaction with the commercially available 4-imidazolecarbaldehyde provided the final product SA16.

Docking calculations. Molecular docking of the OXID-pyridonyl compound SA16 was carried out using the Glide 6.5 program[58]. Ligand structure was first generated through the Maestro sketcher and then prepared through the LigPrep module, as implemented in the Maestro 10.0.013 graphical user interface[59]. The seven receptor structures (PDB codes: 4CEG[38]; 4J8M[40]; 4UYN[39]; 4UZH[39]; 3UOL[42]; 3H10[37]; 2C6E[41]) of AurA and the DFG-out conformation of PDK1 (PDB code: 3NAX)[60] were prepared through the Protein Preparation Wizard, also implemented in Maestro, and the OPLS-2005 force field. Water molecules and residual crystallographic buffer components were removed, missing side chains were built using the Prime module, hydrogen atoms were added, side

chains protonation states at pH 7.0 were assigned and, finally, minimization was performed until the RMSD of all the heavy atoms was within 0.3 Å of the positions determined by X-ray crystallography . In the specific case of the PDK1 DFG-out conformation, the salt bridge between Lys-111 and Glu-130 typical of the DFG-in conformation is disrupted. As Lys-111 is surrounded by several hydrophobic residues, the Protein Preparation Wizard assigned the neutral protonation state to this residue. The binding pocket was identified by placing a cube centered on the inhibitor molecules in complex with Aurora A or PDK1. The inner box size was chosen to be 15 Å in all directions and the size of the outer box was set by choosing a threshold length for the ligand size to be docked of 20 Å. Molecular Docking calculations were performed by means of Glide 6.5 in extra-precision (XP) mode, using GlideScore for ligand ranking. A maximum of 10000 poses per ligand was set to pass to the grid refinement calculation and the best 1000 poses were kept for the energy minimization step. The maximum number of poses per ligand to be outputted was set to 10. Figures were generated using the UCSF-Chimera software package[61].

GBM cell culture and isolation of GSCs. U87MG, U343MG and ANGM-CSS were used as representative GBM cells and cultured as monolayer according to the respective cell line service.

To isolate GSCs from each GBM cell line, approximately 2.0 x 10^6 cells were suspended in a specific serum-free Neural Stem Cell (NSC) medium[32], lacking serum and containing basic fibroblast growth factor (20 ng/ml), epidermal growth factor (20 ng/ml) and B27 supplement (20 µl/ml) [32]. After 5–6 days of culture, the neurospheres were collected, suspended in NSC medium, dissociated into single cells and plated for the experiments.

To characterize spheres isolated from GBM cells, real time PCR and western blotting analyses of stem cells markers were performed (see Supplementary Figure 3). Moreover, cells were assessed for their *clonogenic potential*, using a limiting dilution initiation analysis to quantify, in the GSC and U87MG adherent cells, the frequency of neurospheres-initiation cells (Supplementary Figure 4)[62]. Briefly, the U87MG adherent cells and the GSC were dissociated with trypsin/EDTA and seeded in NSC medium at a density of 1, 5, 10, 50 or 100 cells/well in a 96-multiwell plate. After two weeks of incubation, the formed neurospheres were counted. Wells containing neurospheres (almost exclusively one neurosphere per well) were scored, and the data generated computed using ELDA's online algorithm (http://bioinf.wehi.edu.au/software/elda/).

For the colony formation analysis, GSCs were dissociated and seeded at density of 1 cell/well in NSC medium. Wells that contained a single cell was identified with microscopic observation, and the cells were maintained in NSC medium. After 14 days, colony formation was scored. The

percentage of cells that formed spheres was determined by the following equation: (Y*(n)*/X*(n)*) *100 where X*(n)* is the number of wells in which a single cell was present and Y*(n)* is the number of wells in which one neurosphere developed from a single cell. The mean percentage of wells containing one neurosphere was measured and the mean diameter was evaluated using Image J program.

Isolation and culture of human MSC and T lymphocytes. Human MSCs (Lonza, Milan, Italy), were cultured in the specific growth medium, and maintained at 37 °C in 5% CO_2. Mononuclear cell isolation was assessed according to the method of Boyum[63], as previously reported[64]. MSCs (5 x 10^3 cells/well) or lymphocytes were seeded in 96-multiwell plate and incubated for 72 h with the indicated concentrations of SA16. At the end of treatments, the compound toxicity was verified using the MTS assay, as described below.

Cell proliferation assays of GBM cells and GSCs. The human GBM cells (i.e., U87MG, U343MG or ANGM-CSS) or the respective GSCs were seeded and incubated for the indicated times with the indicated concentrations of SA16 (1 nM-100 μM), MP7[12] or Alisertib[23]. When indicated, cells were treated with MP7 and Alisertib in combination. To verify GSC chemoresistance, U87MG or GSCs were incubated with 50 μM TMZ for 72 h. For the long-term treatment of cells, NSC or complete medium containing drugs was replaced every three days. Cell proliferation was determined using the MTS assay according to manufacturer's instruction[65]: the dehydrogenase activity in active mitochondria reduces 3-(4, 5-dimethylthiazol-2-yl)-5-(3-carboxy methoxyphenyl)-2-(4-sulfophenyl)-2H-tetrazolium (MTS) to the soluble formazan product, whose absorbance at 490 nm was measured with an automated plate reader[65]. The mean background from each test condition was subtracted and the data were expressed as the percentage of untreated cells (control). IC_{50} values were derived from the sigmoid dose-response curve. The percentage of inhibition was calculated as 100 % minus the percentage of cell proliferation.

Counting of viable and dead cells. GBM cells or GSCs were treated as described in the preceding paragraph. Following the treatment period, cell viability was determined using the Muse® Count & Viability Reagent (Merck KGaA, Darmstadt, Germany)[66] according to manufacturer's instruction.

Wound healing migration assay. The U87MG cell monolayer was incubated for 72 h with 10 μM SA16. The cells were then scratched as described[10], and images of the closure of the scratch were captured at 0, 6, and 24 h.

Apoptosis assessment

U87MG or GSCs were incubated with SA16 for 72 h or 7 days, respectively. Following treatment, early and late apoptotic cells were distinguished by using the annexin V conjugated with fluorescein isothiocyanate (FITC) and amino-actinomycin D (7-AAD), using the Muse Apo Assays® (Merck-Millipore) as reported before[67].

RNA extraction and real time PCR analysis

U87MG or GSCs were incubated with SA16 for 72 h or 7 days, respectively. The mRNA levels of Nestin, MAP2 and GFAP were evaluated by quantitative real time PCR using Fluocycle® II SYBR® (Euroclone, Milan, Italy)[68]. The nucleotide sequences, annealing temperature and product size of the primers have been previously reported[69].

Quantification of the occupied area and the cellular processes of neurospheres. GSCs isolated from U87MG cells were plated in complete medium and treated for seven days with different concentration of SA16, MP7, Alisertib or a combination of MP7 and Alisertib. At the end of the treatment period, images were captured, and the area occupied by neurospheres that had formed, as well as the length of cellular processes were quantified as described[32]. Five different wells were analysed for each condition, with 15 images captured for each well[32]. Cellular processes were measured considering the average diameter of an individual neurosphere in the vertical and horizontal planes, and the neurite lengths were measured according to literature protocols[32, 70].

Colony forming assay. The self-renewal capability was assessed with the soft-agar colony forming assays[66]. Briefly, GSCs were dissociated, and 500 μl of $1x10^4$ cells/ml were suspended in NSC medium containing 0.3% agar (low melting temperature agarose, Sigma-Aldrich, Milan, Italy). 500 μl of the obtained suspension were treated with SA16 and were plated on a layer of 500 μl of the same medium containing 0.6% agar in a 24 well plate. The plates were fed weekly with 0.1 ml of NSC medium. Three weeks after plating, the photographs of the colonies were taken. The number of colonies derived by a single cell was evaluated and the images were analysed using Image J program.

Western blotting analysis. U87MG or GSCs were incubated with DMSO (control), or SA16 (10 μM) for 72 h or seven days, respectively. At the end of the treatment periods, the cells were collected and lysed[32]. Cell extracts were resolved using SDS-PAGE, and the amount of proteins were detected using the primary antibodies described in Daniele, S.[32]. The Image J Software was used to perform the densitometric analysis of immunoreactive bands.

Statistical analysis. Graph-Pad Prism (GraphPad Software Inc., San Diego, CA) was used for data analysis and graphic presentations. All data are presented as the mean ± SEM. One-way analysis of variance (ANOVA) with Bonferroni's corrected t-test for post-hoc pair-wise comparisons was used to perform statistical analysis.

Supporting information

Characterization of GSCs derived from U87MG cells, proliferation and viability experiments on U87MG, U343MG and ANGM-CSS cells, and results from SelectScreen™ Kinase Profiling Service for SA16, selection of receptor conformations for docking and crystallographic parameters of the analyzed AurA structures, synthetic scheme of SA16.

ABBREVIATIONS

GBM, Glioblastoma Multiforme

GSCs, Glioblastoma cancer stem cells

PDK1, Phosphoinositide-dependent kinase-1

AurA, Aurora A

MSCs, mesenchymal stem cells

Author Contributions

S.D. performed biological experiments and wrote the manuscript. S.S. synthesized the compounds and helped in writing the manuscript too. D.P. and C.G. performed experiments in GSCs and analysed the data; D.D.M performed molecular docking calculations; S.R., G.C., E.N and L.M. designed the study and played a key role as project supervisor. S.R. and C.M coordinated the project. All the authors contributed to and approved the final manuscript.

Funding sources

The study was supported by the International Society of Drug Discovery S.r.l. (ISDD, Milan), by FIRB, Bando Futuro in Ricerca 2010 (Grant RBFR10ZJQT), by the University of Pisa (PRA_2016_59), and by PRIN2015FCHJ8E_004.

Conflict of Interest

The authors declare no competing financial interest.

Acknowledgment

We thank Dr. Elisa Mimì Zappelli for her valuable advice with neurospheres.

Figures

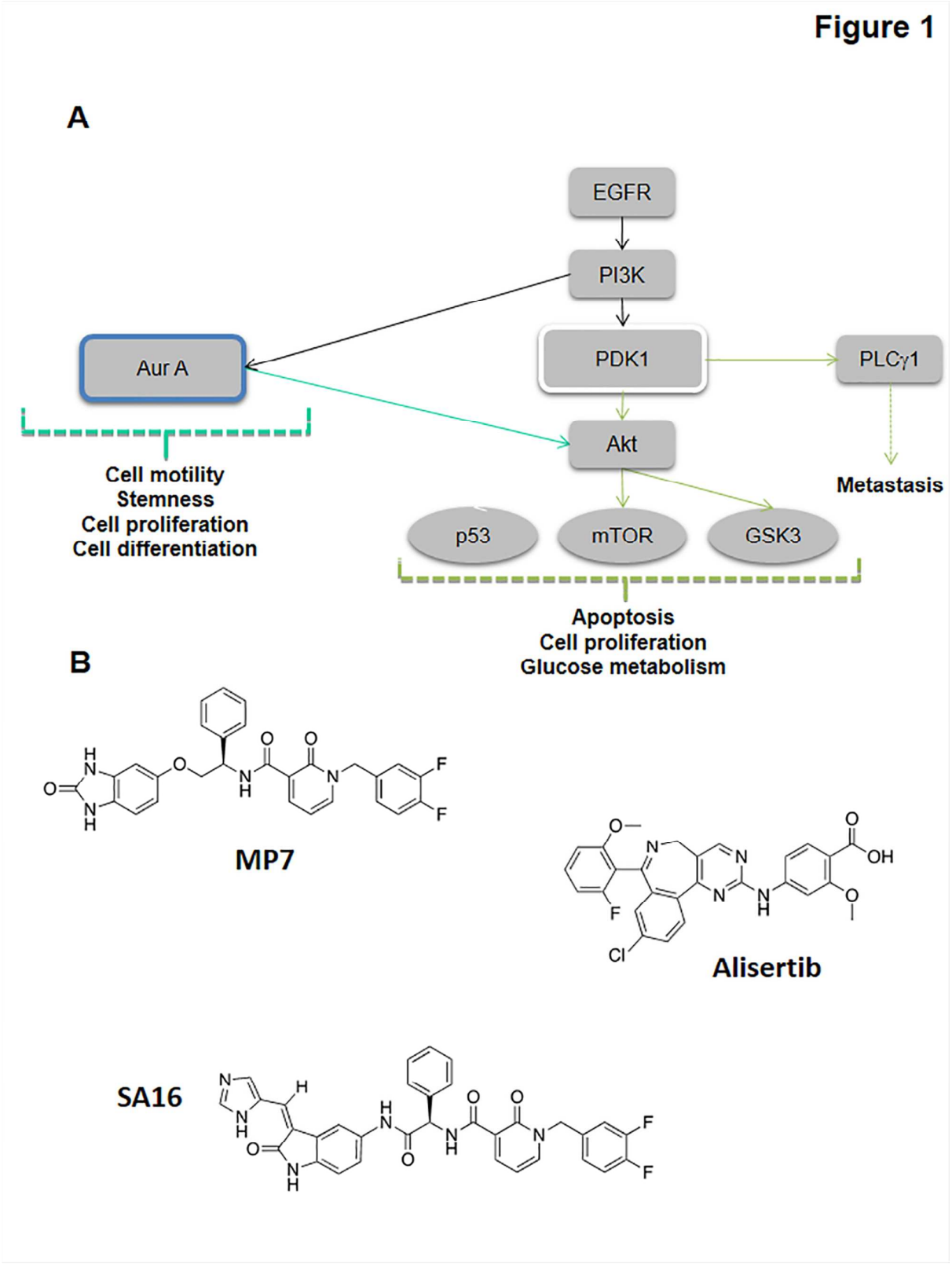
Figure 1
A
EGFR
PI3K
Aur A
PDK1
PLCγ1
Akt
Cell motility
Stemness
Cell proliferation
Cell differentiation
Metastasis
p53
mTOR
GSK3
Apoptosis
Cell proliferation
Glucose metabolism
B
MP7
Alisertib
SA16

Figure 2

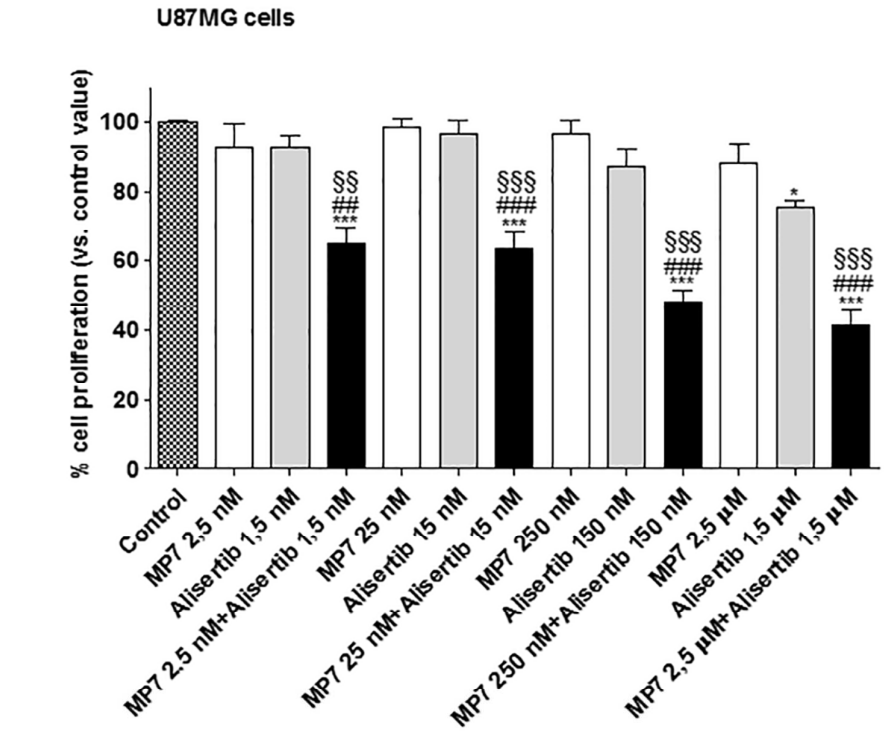
A
U87MG cells
% cell prolferation (vs. control value)
Control
MP7 2,5 nM
Alisertib 1,5 nM
MP7 2,5 nM+Alisertib 1,5 nM
MP7 25 nM
Alisertib 15 nM
MP7 25 nM+Alisertib 15 nM
MP7 250 nM
Alisertib 150 nM
MP7 250 nM+Alisertib 150 nM
MP7 2,5 µM
Alisertib 1,5 µM
MP7 2,5 µM+Alisertib 1,5 µM

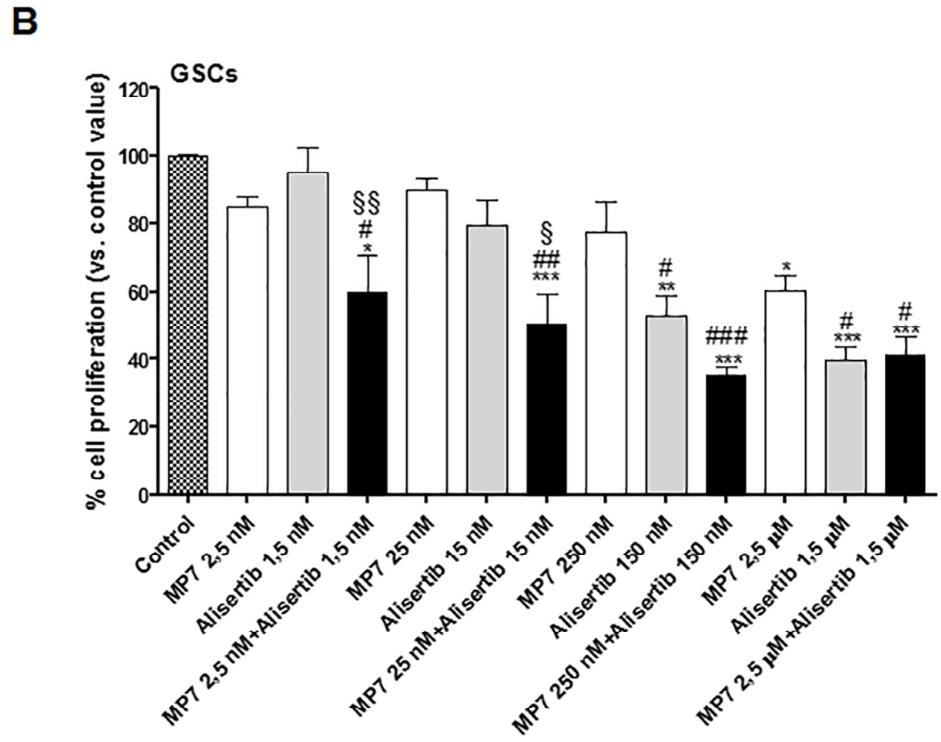
B
GSCs
% cell proliferation (vs. control value)
Control
MP7 2,5 nM
Alisertib 1,5 nM
MP7 2,5 nM+Alisertib 1,5 nM
MP7 25 nM
Alisertib 15 nM
MP7 25 nM+Alisertib 15 nM
MP7 250 nM
Alisertib 150 nM
MP7 250 nM+Alisertib 150 nM
MP7 2,5 µM
Alisertib 1,5 µM
MP7 2,5 µM+Alisertib 1,5 µM

Figure 3

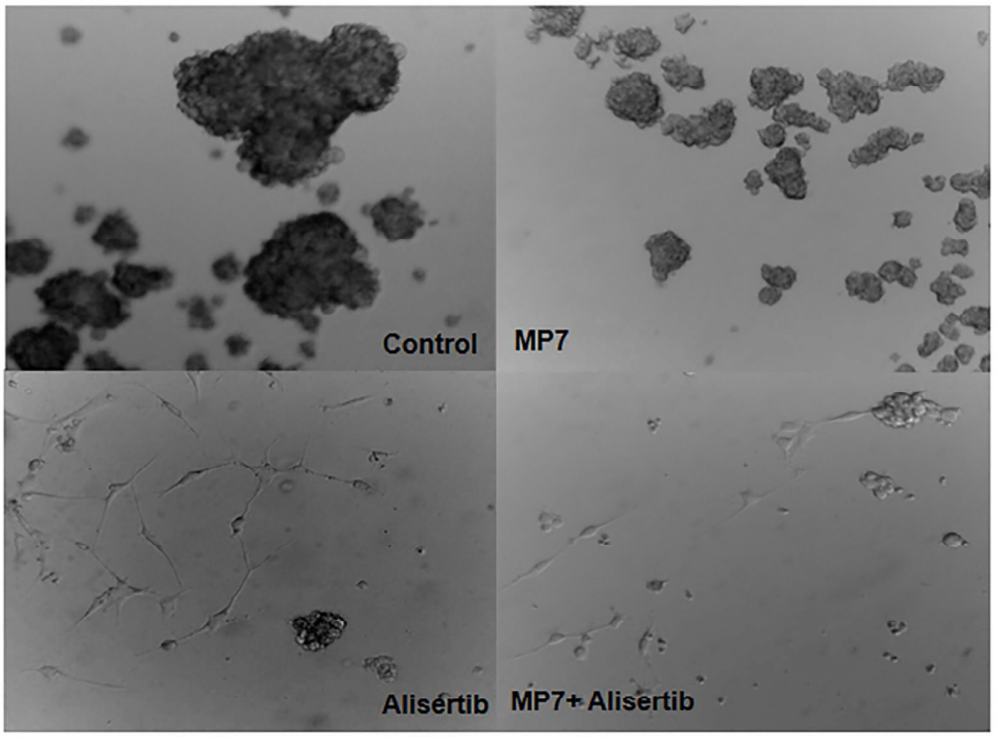
A
Control
MP7
Alisertib
MP7+ Alisertib

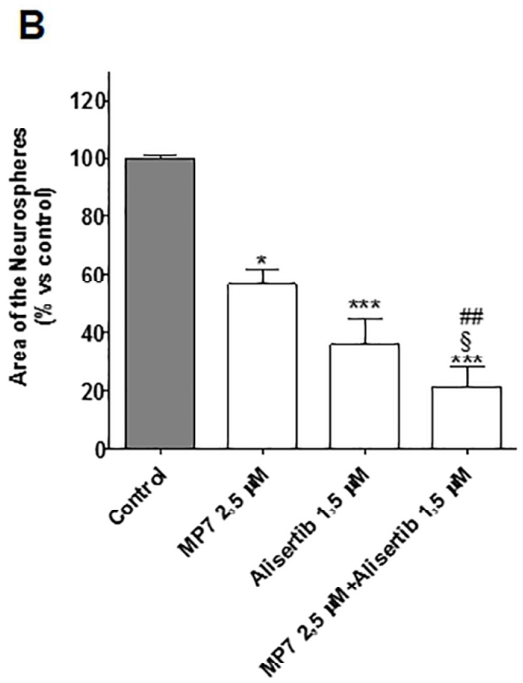
B
Area of the Neurospheres (% vs control)
120
100
80
60
40
20
0
*
***
##
§
***
Control
MP7 2,5 µM
Alisertib 1,5 µM
MP7 2,5 µM+Alisertib 1,5 µM

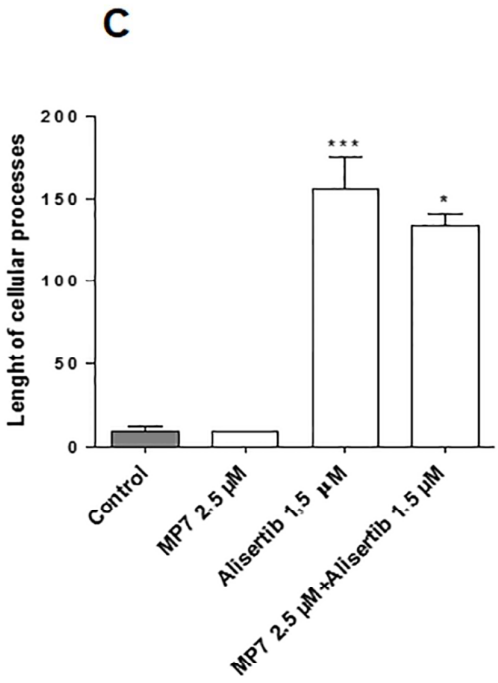
C
Lenght of cellular processes
200
150
100
50
0
***
*
Control
MP7 2,5 µM
Alisertib 1,5 µM
MP7 2,5 µM+Alisertib 1,5 µM

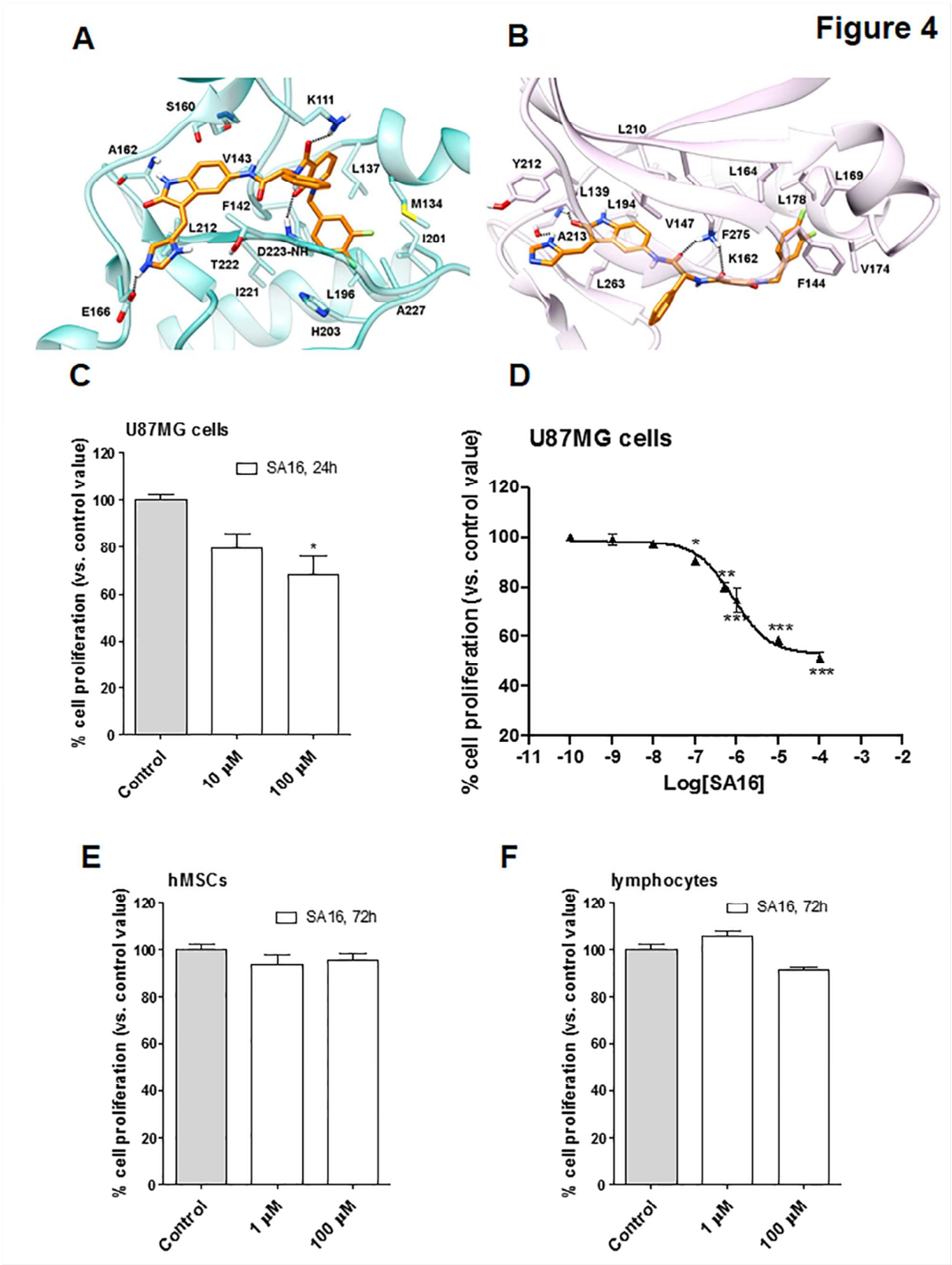
Figure 4
A
S160
K111
A162
V143
L137
F142
M134
L212
I201
D223-NH
T222
I221
L196
E166
A227
H203
B
L210
Y212
L164
L169
L139
L194
L178
V147
A213
F275
K162
V174
L263
F144
C
U87MG cells
SA16, 24h
% cell proliferation (vs. control value)
Control
10 μM
100 μM
D
U87MG cells
% cell proliferation (vs. control value)
Log[SA16]
E
hMSCs
SA16, 72h
% cell proliferation (vs. control value)
Control
1 μM
100 μM
F
lymphocytes
SA16, 72h
% cell proliferation (vs. control value)
Control
1 μM
100 μM

Figure 5

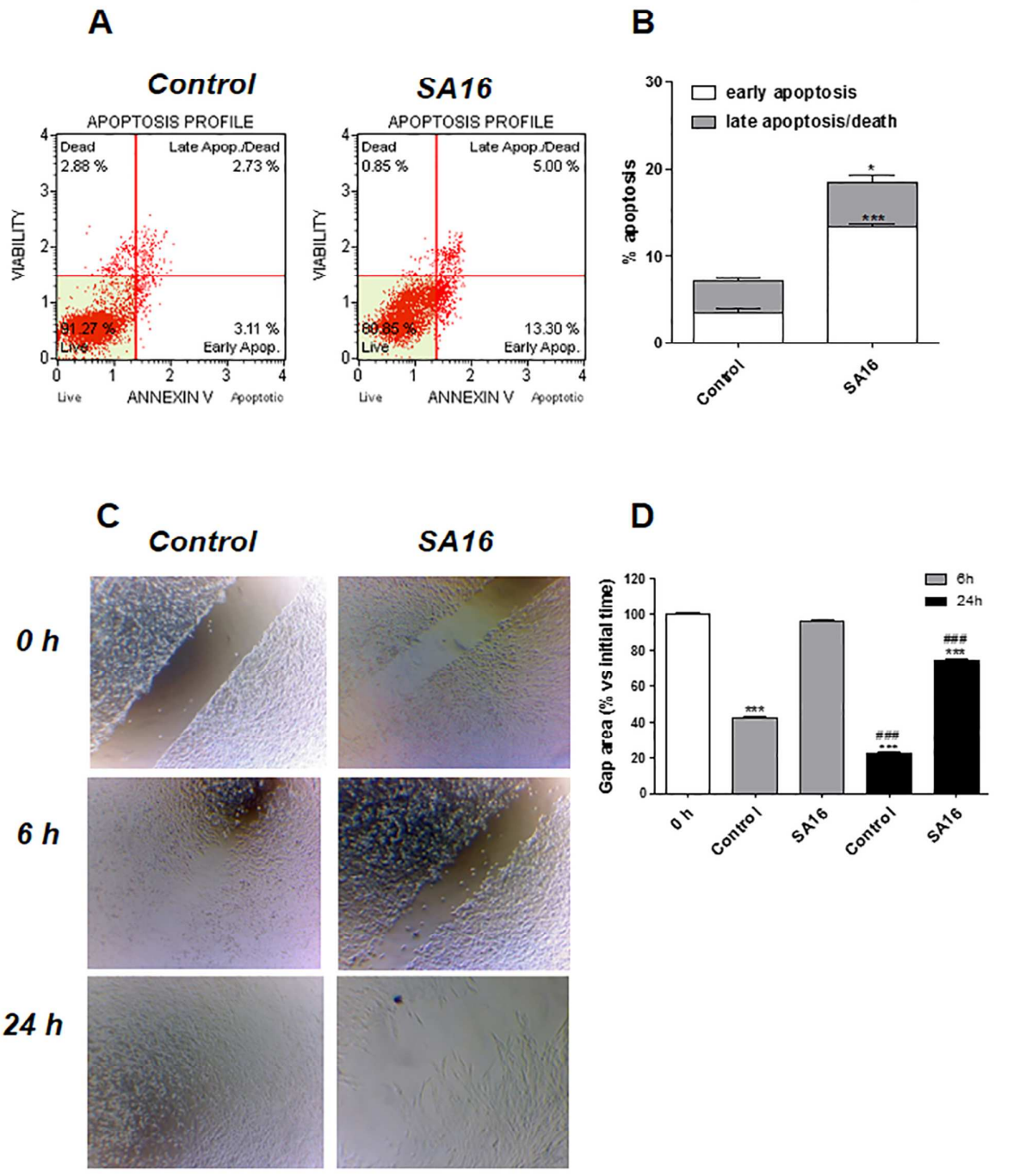
A
Control
SA16
APOPTOSIS PROFILE
Dead
2.88 %
Late Apop./Dead
2.73 %
91.27 %
Live
3.11 %
Early Apop.
VIABILITY
ANNEXIN V
Live
Apoptotic
Dead
0.85 %
Late Apop./Dead
5.00 %
80.85 %
Live
13.30 %
Early Apop.
B
early apoptosis
late apoptosis/death
% apoptosis
Control
SA16
C
Control
SA16
0 h
6 h
24 h
D
6h
24h
Gap area (% vs initial time)
0 h
Control
SA16
Control
SA16

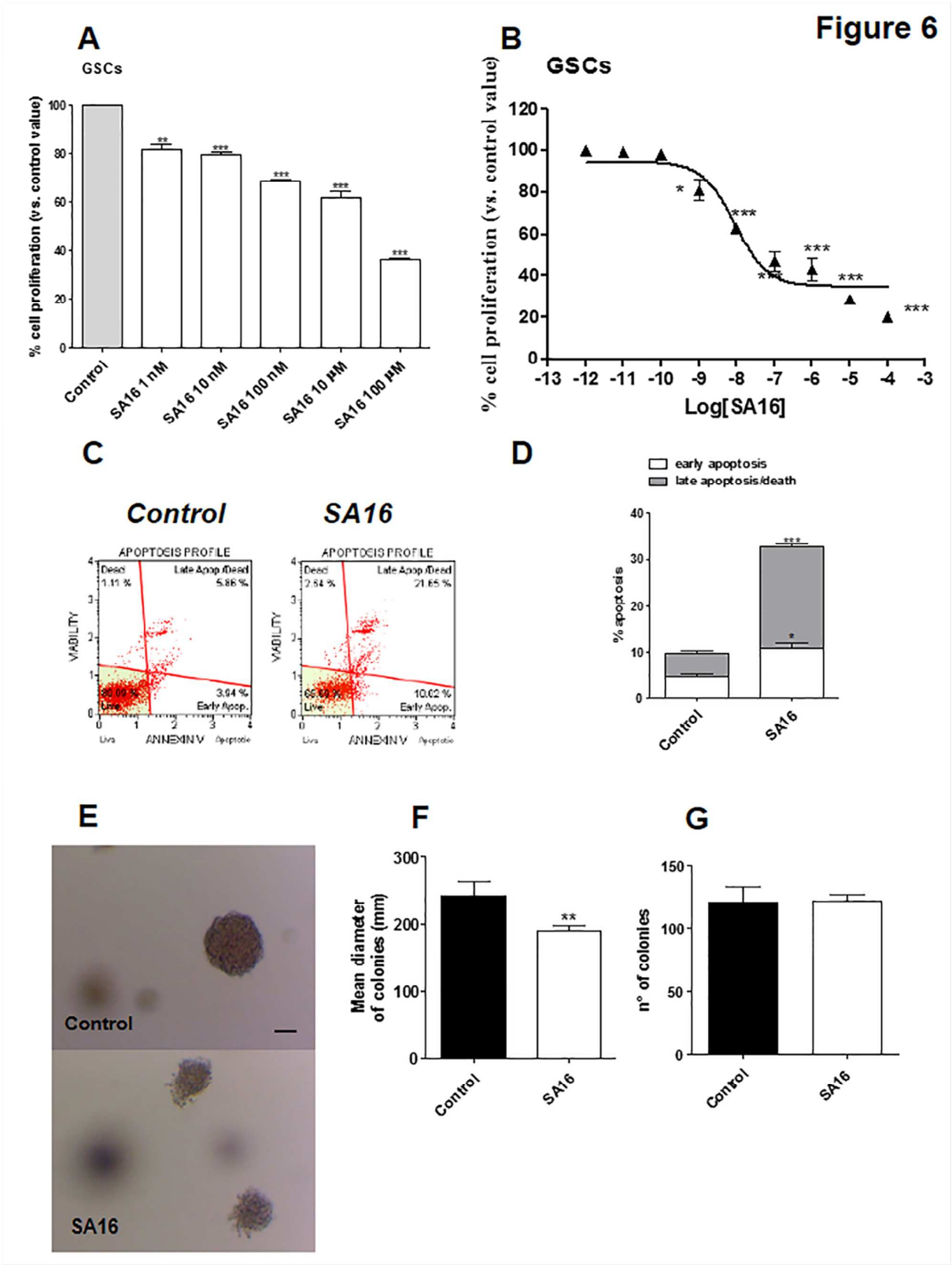
Figure 6
A
GSCs
% cell proliferation (vs. control value)
Control
SA16 1 nM
SA16 10 nM
SA16 100 nM
SA16 10 µM
SA16 100 µM
B
GSCs
% cell proliferation (vs. control value)
Log[SA16]
C
Control
SA16
APOPTOSIS PROFILE
VIABILITY
ANNEXIN V
Dead
Late Apop./Dead
Live
Early Apop.
D
early apoptosis
late apoptosis/death
% apoptosis
Control
SA16
E
Control
SA16
F
Mean diameter of colonies (mm)
Control
SA16
G
n° of colonies
Control
SA16

Figure 7

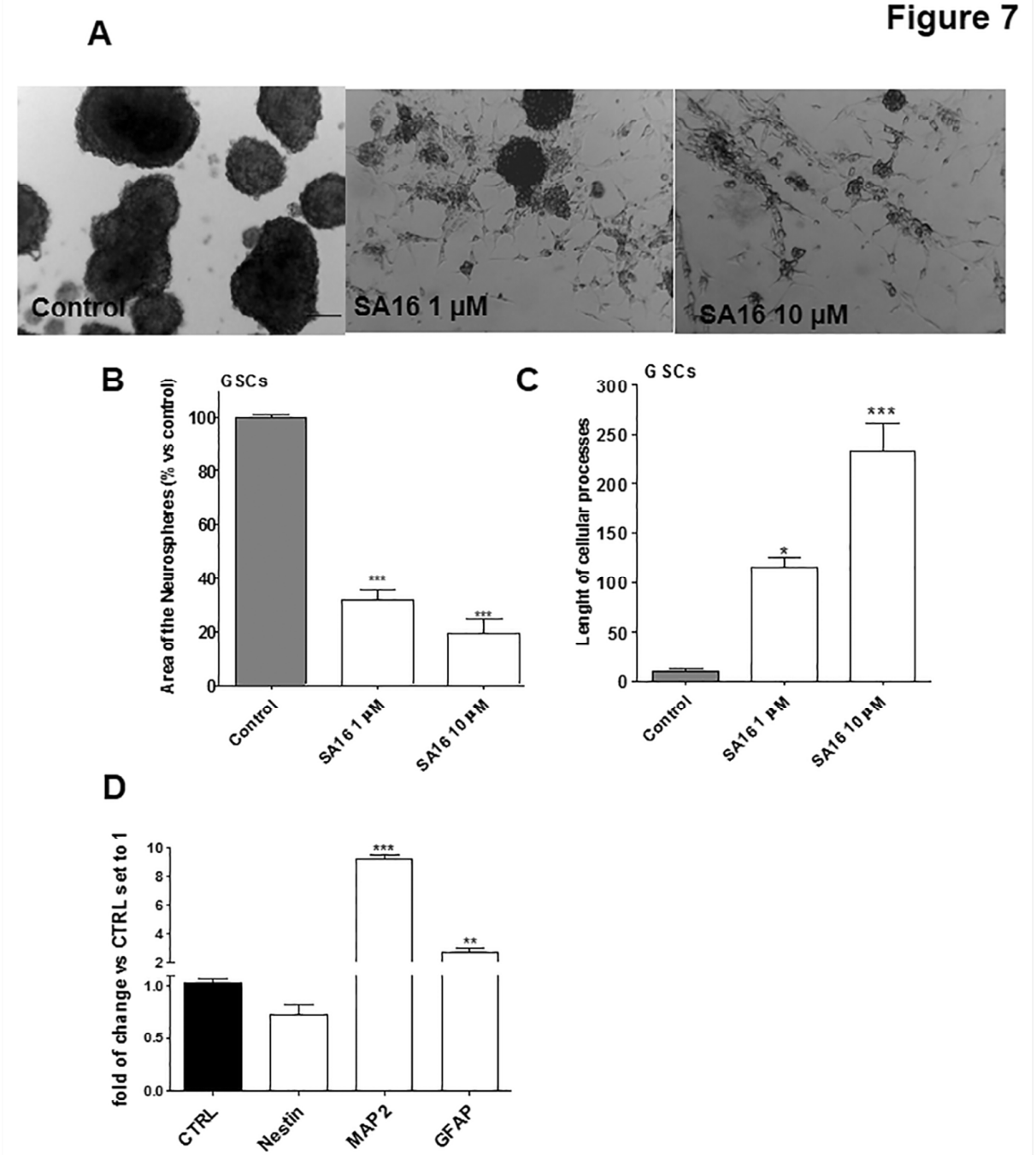
A
Control
SA16 1 µM
SA16 10 µM
B
GSCs
Area of the Neurospheres (% vs control)
100
80
60
40
20
0
***
***
Control
SA16 1 µM
SA16 10 µM
C
G SCs
Lenght of cellular processes
300
250
200
150
100
50
0
*
***
Control
SA16 1 µM
SA16 10 µM
D
fold of change vs CTRL set to 1
10
8
6
4
2
1.0
0.5
0.0
***
**
CTRL
Nestin
MAP2
GFAP

Figure 8

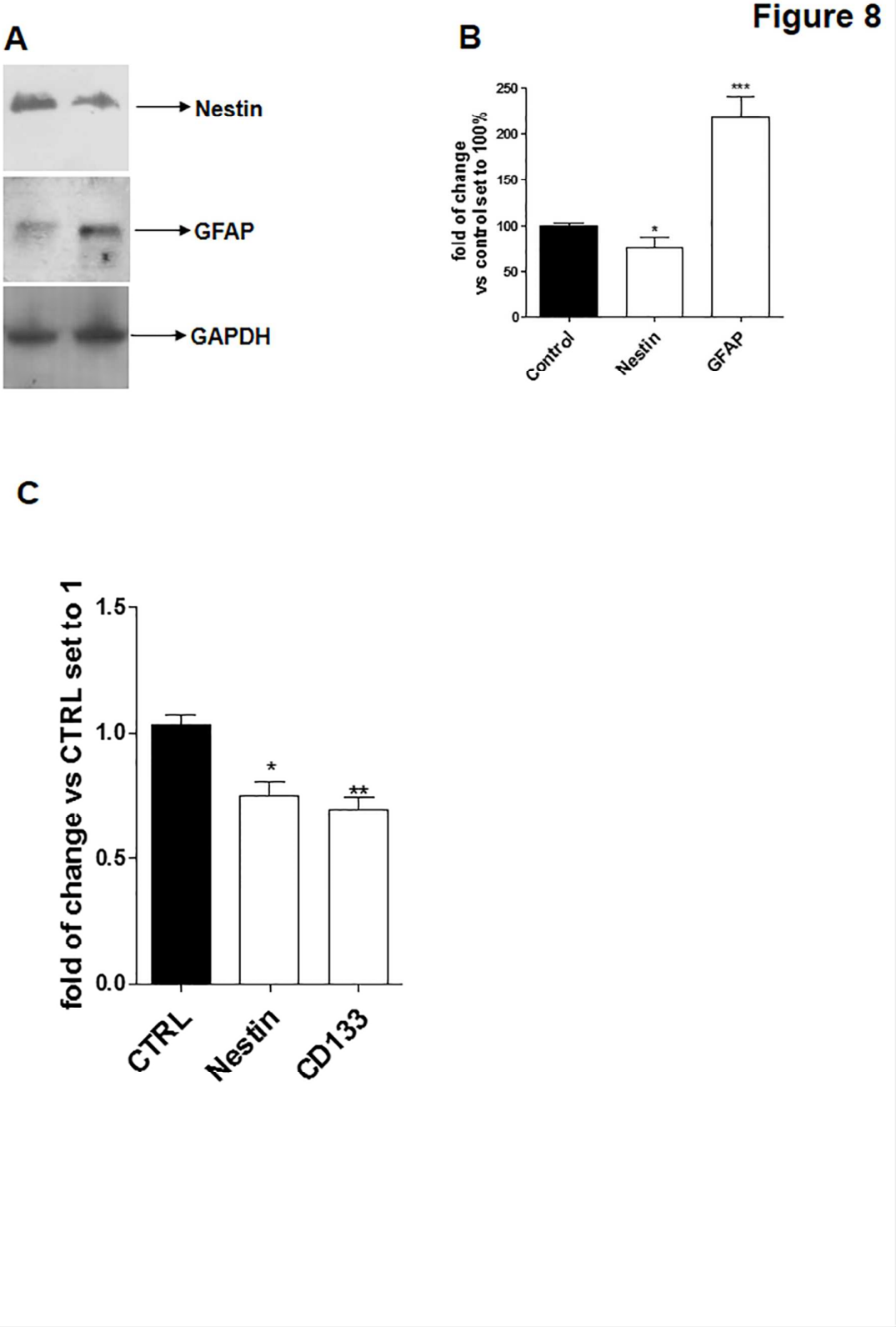
A
Nestin
GFAP
GAPDH
B
fold of change vs control set to 100%
250
200
150
100
50
0
*
***
Control
Nestin
GFAP
C
fold of change vs CTRL set to 1
1.5
1.0
0.5
0.0
*
**
CTRL
Nestin
CD133

Figure Legends

Fig. 1. (A) Crosstalk between the PDK1/AurA pathways. PDK1 phosphorilates Akt and Phospholipase C-Gamma 1 (PLCγ1), influencing apoptosis, cell proliferation, glucose metabolism and metastasis formation. Akt activity is also influenced by AurA. Aberrant AurA activity induces cell motility, cell stemnsess, proliferation and differentiation. PI3K, which activates the PDK1/Akt pathway, can influence AurA effect too. **(B)** Chemical formulas of MP7, Alisertib and SA16.

Fig. 2. Effects of PDK1 and AurA inhibition on GBM and GSC proliferation. **(A, B)** U87MG cells (A) or GSCs (B) were incubated with the indicated concentrations of the PDK1 inhibitor MP7 or the AurA inhibitor Alisertib, alone or in combination, for 72 h or seven days, respectively. At the end of treatment, cell proliferation was evaluated as described in the Methods Section. The data are expressed as a percentage with respect to that of untreated cells (control), which was set to 100% (mean values ± SEM, N = 3). * $p<0.05$, ** $p<0.01$, *** $p<0.001$ vs. control cells; # $p<0.05$, ## $p<0.01$, ### $p<0.001$ vs cells treated with MP7 alone; § $p<0.05$, §§ $p<0.01$, §§§ $p<0.001$ vs cells treated with Alisertib alone.

Fig. 3. Effects of PDK1 and AurA inhibition on GSC morphology. **(A-C)** GSCs were incubated with complete medium containing DMSO (control), 2,5 μM MP7 and 1,5 μM Alisertib, alone or in combination, for seven days. (A) Representative cell micrographs after seven days of treatment are shown. The area of the culture plates occupied by the spheres (B) and the length of cellular processes (C) were scored after seven days of treatment (mean values ± SEM, N = 3). * $p<0.05$, *** $p<0.001$ vs. control, ## $p<0.01$ vs MP7 alone, § $p<0.05$ vs Alisertib alone.

Fig. 4. (**A, B**) Binding mode of SA16 as found by the docking calculations within its A) PDK1 and B) AurA biding sites. Both SA16 (colored in orange) and the protein residues involved into binding are depicted as sticks. The structures of PDK1 and AurA are depicted as cartoons, colored in cyan and pink, respectively. **(C, D)** U87MG cells were treated in complete medium with the indicated concentrations of SA16 for 24 h (C) or 72 h (D), and cell proliferation was evaluated as described in the Methods Section. **(E, F)** Human MSCs (E) or lymphocytes (F) were treated with DMSO or the indicated SA16 concentrations. Following treatment, cell proliferation was evaluated as described in the Methods section. The data are expressed as a percentage with respect to that of untreated cells (control), which was set to 100% (mean values ± SEM, N = 3). * $p<0.05$, ** $p<0.01$, *** $p<0.001$ vs. control.

Fig. 5. SA16 induces GBM cell apoptosis and inhibits cell migration. **(A, B)** U87MG cells were incubated with DMSO (control), or 10 μM SA16 for 72 h. At the end of the treatment period, the cells were collected, and the level of phosphatidylserine externalisation was evaluated using the Annexin V-staining protocol. (B) The data are expressed as the percentage of apoptotic cells versus the total number of cells (mean values ± SEM, N = 3). The data for the early-stage apoptotic cells are shown in white, while the data for the late-stage apoptotic/necrotic cells are shown in grey. * $p<0.05$, *** $p<0.001$ vs. control. **(C, D)** U87MG cells were treated for 72 h with DMSO (control), or 10 μM SA16. Following treatment, the cell monolayer was scratched (time zero), and cells were grown in fresh medium. Representative micrographs were taken after 6 h and 24 h from the scratch (C). The gap area (D) was measured after 6 h and 24 h from the scratch (mean values ± SEM, N = 3). *** $p<0.001$ vs control; ### $p<0.001$ vs respective gap area at 6 h from the scratch.

Fig. 6. SA16 induces GSC apoptosis and blocks GSC formation **(A, B)** U87MG-derived GSCs were incubated with different concentrations of SA16 for four days (A) or seven days (B). At the end of treatment, cell proliferation was evaluated as described in the Methods Section. **(C, D)** GSCs were treated as in B, and the apoptosis degree was evaluated using the Annexin V protocol. (C) The data were expressed as the percentage of apoptotic cells (early-apoptotic is represented in white, late-apoptotic/necrotic in grey) relative to the total number of cells (mean values ± SEM, N = 3). **(E-G)** For the soft-agar assay the GSC cells were treated with DMSO or SA16 (1 nM) in NSC medium for 21 days. (**E**) Representative pictures of the cells after 21 days of incubation were shown. The mean diameter (**F**) and the number of the newly formed spheres (**G**) were scored. * $p<0.05$, ** $p<0.01$, *** $p<0.001$ vs. control.

Fig. 7. SA16 induces GSC differentiation. GSCs were incubated for seven days with complete medium containing DMSO (control), or the indicated concentrations of SA16. (A) Representative cell micrographs after seven days of treatment are shown. The area occupied by the cells in culture plates (B) and the outgrowth of cellular processes (C) were scored after seven days of treatment (mean values ± SEM, N = 3). (D) Total RNA was extracted and the relative mRNA quantification of the stem cell marker Nestin, the neuronal marker MAP2 and the astrocyte marker GFAP was performed by RT-PCR. The data are expressed as the fold change vs. the levels of the control (mean values ± SEM, N = 3). * $p<0.05$, **$p<0.01$, *** $p<0.001$ vs. control.

Fig. 8. SA16 reduces GBM stemness potential (**A, B**) GSCs were treated with DMSO (control) or 10 μM SA16 for seven days; the protein levels of the stemness marker Nestin and of the glial marker GFAP were assessed by Western blotting, using GAPDH as the loading control. **(C)** U87MG were incubated with SA16 for 72 h. (C) Total RNA was extracted and the relative mRNA quantification of the stem cell markers Nestin and CD133 was performed by RT-PCR. The data are expressed as the fold change vs. the levels of the control (mean values ± SEM, N = 3). * $p<0.05$, ** $p<0.01$, *** $p<0.001$ vs. control.

References

1. Olar, A., and Aldape, K. D. (2014) Using the molecular classification of glioblastoma to inform personalized treatment, *The Journal of pathology 232*, 165-177.
2. Ostrom, Q. T., Gittleman, H., Farah, P., Ondracek, A., Chen, Y., Wolinsky, Y., Stroup, N. E., Kruchko, C., and Barnholtz-Sloan, J. S. (2013) CBTRUS statistical report: Primary brain and central nervous system tumors diagnosed in the United States in 2006-2010, *Neuro-oncology 15*, ii1-ii56.
3. Eramo, A., Ricci-Vitiani, L., Zeuner, A., Pallini, R., Lotti, F., Sette, G., Pilozzi, E., Larocca, L., Peschle, C., and De Maria, R. (2006) Chemotherapy resistance of glioblastoma stem cells, *Cell Death & Differentiation 13*, 1238-1241.
4. Signore, M., Pelacchi, F., Di Martino, S., Runci, D., Biffoni, M., Giannetti, S., Morgante, L., De Majo, M., Petricoin, E., and Stancato, L. (2014) Combined PDK1 and CHK1 inhibition is required to kill glioblastoma stem-like cells in vitro and in vivo, *Cell Death and Disease 5*, e1223.
5. Peifer, C., and Alessi, D. R. (2008) Small‐Molecule Inhibitors of PDK1, *ChemMedChem 3*, 1810-1838.
6. Choi, J. H., Yang, Y. R., Lee, S. K., Kim, S. H., Kim, Y. H., Cha, J. Y., Oh, S. W., Ha, J. R., Ryu, S. H., and Suh, P. G. (2008) Potential inhibition of PDK1/Akt signaling by phenothiazines suppresses cancer cell proliferation and survival, *Annals of the New York Academy of Sciences 1138*, 393-403.
7. Gagliardi, P. A., di Blasio, L., and Primo, L. (2015) PDK1: A signaling hub for cell migration and tumor invasion, *Biochimica et Biophysica Acta (BBA)-Reviews on Cancer 1856*, 178-188.
8. Courtney, K. D., Corcoran, R. B., and Engelman, J. A. (2010) The PI3K pathway as drug target in human cancer, *Journal of Clinical Oncology 28*, 1075-1083.
9. Sestito, S., Nesi, G., Daniele, S., Martelli, A., Digiacomo, M., Borghini, A., Pietra, D., Calderone, V., Lapucci, A., Falasca, M., Parrella, P., Notarangelo, A., Breschi, M. C., Macchia, M., Martini, C., and Rapposelli, S. (2015) Design and synthesis of 2-oxindole based multi-targeted inhibitors of PDK1/Akt signaling pathway for the treatment of glioblastoma multiforme, *European Journal of Medicinal Chemistry 105*, 274-288.
10. Sestito, S., Daniele, S., Nesi, G., Zappelli, E., Di Maio, D., Marinelli, L., Digiacomo, M., Lapucci, A., Martini, C., Novellino, E., and Rapposelli, S. (2016) Locking PDK1 in DFG-out conformation through 2-oxo-indole containing molecules: Another tools to fight glioblastoma, *Eur J Med Chem 118*, 47-63.
11. Lassman, A. B., Abrey, L. E., and Gilbert, M. R. (2006) Response of glioblastomas to EGFR kinase inhibitors, *N Engl J Med 354*, 525-526.
12. Nagashima, K., Shumway, S. D., Sathyanarayanan, S., Chen, A. H., Dolinski, B., Xu, Y., Keilhack, H., Nguyen, T., Wiznerowicz, M., and Li, L. (2011) Genetic and Pharmacological Inhibition of PDK1 in Cancer Cells CHARACTERIZATION OF A SELECTIVE ALLOSTERIC KINASE INHIBITOR, *Journal of Biological Chemistry 286*, 6433-6448.
13. Tamgüney, T., Zhang, C., Fiedler, D., Shokat, K., and Stokoe, D. (2008) Analysis of 3-phosphoinositide-dependent kinase-1 signaling and function in ES cells, *Experimental cell research 314*, 2299-2312.
14. Kesari, S. (2011) Understanding glioblastoma tumor biology: the potential to improve current diagnosis and treatments, In *Seminars in oncology*, pp S2-S10, Elsevier.
15. Holohan, C., Van Schaeybroeck, S., Longley, D. B., and Johnston, P. G. (2013) Cancer drug resistance: an evolving paradigm, *Nature Reviews Cancer 13*, 714-726.
16. Tao, L., Zhu, F., Xu, F., Chen, Z., Jiang, Y. Y., and Chen, Y. Z. (2015) Co-targeting cancer drug escape pathways confers clinical advantage for multi-target anticancer drugs, *Pharmacological research 102*, 123-131.
17. Turner, N. C., and Reis-Filho, J. S. (2012) Genetic heterogeneity and cancer drug resistance, *The lancet oncology 13*, e178-e185.
18. Galli, R., Binda, E., Orfanelli, U., Cipelletti, B., Gritti, A., De Vitis, S., Fiocco, R., Foroni, C., Dimeco, F., and Vescovi, A. (2004) Isolation and characterization of tumorigenic, stem-like neural precursors from human glioblastoma, *Cancer research 64*, 7011-7021.

19. Bao, S., Wu, Q., McLendon, R. E., Hao, Y., Shi, Q., Hjelmeland, A. B., Dewhirst, M. W., Bigner, D. D., and Rich, J. N. (2006) Glioma stem cells promote radioresistance by preferential activation of the DNA damage response, *Nature 444*, 756-760.
20. Happold, C., Roth, P., Wick, W., Schmidt, N., Florea, A. M., Silginer, M., Reifenberger, G., and Weller, M. (2012) Distinct molecular mechanisms of acquired resistance to temozolomide in glioblastoma cells, *Journal of neurochemistry 122*, 444-455.
21. Fan, X., Khaki, L., Zhu, T. S., Soules, M. E., Talsma, C. E., Gul, N., Koh, C., Zhang, J., Li, Y. M., and Maciaczyk, J. (2010) NOTCH pathway blockade depletes CD133 - positive glioblastoma cells and inhibits growth of tumor neurospheres and xenografts, *Stem cells 28*, 5-16.
22. Kim, K. H., Seol, H. J., Kim, E. H., Rheey, J., Jin, H. J., Lee, Y., Joo, K. M., Lee, J., and Nam, D.-H. (2012) Wnt/β-catenin signaling is a key downstream mediator of MET signaling in glioblastoma stem cells, *Neuro-oncology*, nos299.
23. Hong, X., O'Donnell, J. P., Salazar, C. R., Van Brocklyn, J. R., Barnett, K. D., Pearl, D. K., Ecsedy, J. A., Brown, S. L., Mikkelsen, T., and Lehman, N. L. (2014) The selective Aurora-A kinase inhibitor MLN8237 (alisertib) potently inhibits proliferation of glioblastoma neurosphere tumor stem-like cells and potentiates the effects of temozolomide and ionizing radiation, *Cancer chemotherapy and pharmacology 73*, 983-990.
24. Yang, S., He, S., Zhou, X., Liu, M., Zhu, H., Wang, Y., Zhang, W., Yan, S., Quan, L., and Bai, J. (2010) Suppression of Aurora-A oncogenic potential by c-Myc downregulation, *Experimental & molecular medicine 42*, 759-767.
25. Lehman, N. L., O'Donnell, J. P., Whiteley, L. J., Stapp, R. T., Lehman, T. D., Roszka, K. M., Schultz, L. R., Williams, C. J., Mikkelsen, T., and Brown, S. L. (2012) Aurora A is differentially expressed in gliomas, is associated with patient survival in glioblastoma and is a potential chemotherapeutic target in gliomas, *Cell Cycle 11*, 489-502.
26. Silva, A., Wang, J., Lomahan, S., Tran, T.-A., Grenlin, L., Suganami, A., Tamura, Y., and Ikegaki, N. (2014) Aurora kinase A is a possible target of OSU-03012 to destabilize MYC family proteins, *Oncology reports 32*, 901-905.
27. Wang, S. I., Puc, J., Li, J., Bruce, J. N., Cairns, P., Sidransky, D., and Parsons, R. (1997) Somatic mutations of PTEN in glioblastoma multiforme, *Cancer research 57*, 4183-4186.
28. Daniele, S., Costa, B., Zappelli, E., Da Pozzo, E., Sestito, S., Nesi, G., Campiglia, P., Marinelli, L., Novellino, E., Rapposelli, S., and Martini, C. (2015) Combined inhibition of AKT/mTOR and MDM2 enhances Glioblastoma Multiforme cell apoptosis and differentiation of cancer stem cells, *Scientific Reports 5*.
29. Erlanson, D. A., Arndt, J. W., Cancilla, M. T., Cao, K., Elling, R. A., English, N., Friedman, J., Hansen, S. K., Hession, C., Joseph, I., Kumaravel, G., Lee, W. C., Lind, K. E., McDowell, R. S., Miatkowski, K., Nguyen, C., Nguyen, T. B., Park, S., Pathan, N., Penny, D. M., Romanowski, M. J., Scott, D., Silvian, L., Simmons, R. L., Tangonan, B. T., Yang, W., and Sun, L. (2011) Discovery of a potent and highly selective PDK1 inhibitor via fragment-based drug discovery, *Bioorganic & medicinal chemistry letters 21*, 3078-3083.
30. Sells, T. B., Chau, R., Ecsedy, J. A., Gershman, R. E., Hoar, K., Huck, J., Janowick, D. A., Kadambi, V. J., LeRoy, P. J., and Stirling, M. (2015) MLN8054 and alisertib (MLN8237): discovery of selective oral aurora A inhibitors, *ACS medicinal chemistry letters 6*, 630-634.
31. Pei, J., Moon, K.-S., Pan, S., Lee, K.-H., Ryu, H.-H., Jung, T.-Y., Kim, I.-Y., Jang, W.-Y., Jung, C.-H., and Jung, S. (2014) Proteomic Analysis between U87MG and U343MG-a cell lines: searching for candidate proteins for glioma invasion, *Brain Tumor Research and Treatment 2*, 22-28.
32. Daniele, S., Zappelli, E., Natali, L., Martini, C., and Trincavelli, M. (2014) Modulation of A1 and A2B adenosine receptor activity: a new strategy to sensitise glioblastoma stem cells to chemotherapy, *Cell death & disease 5*, e1539.
33. Piccirillo, S., Reynolds, B. A., Zanetti, N., Lamorte, G., Binda, E., Broggi, G., Brem, H., Olivi, A., Dimeco, F., and Vescovi, A. L. (2006) Bone morphogenetic proteins inhibit the tumorigenic potential of human brain tumour-initiating cells, *Nature 444*, 761-765.

34. Tan, J., Li, Z., Lee, P. L., Guan, P., Aau, M. Y., Lee, S. T., Feng, M., Lim, C. Z., Lee, E. Y. J., and Wee, Z. N. (2013) PDK1 signaling toward PLK1–MYC activation confers oncogenic transformation, tumor-initiating cell activation, and resistance to mTOR-targeted therapy, *Cancer discovery 3*, 1156-1171.
35. Mannino, M., Gomez-Roman, N., Hochegger, H., and Chalmers, A. J. (2014) Differential sensitivity of Glioma stem cells to Aurora kinase A inhibitors: implications for stem cell mitosis and centrosome dynamics, *Stem cell research 13*, 135-143.
36. Long, Z.-J., Wang, L.-X., Zheng, F.-M., Chen, J.-J., Luo, Y., Tu, X.-X., Lin, D.-J., Lu, G., and Liu, Q. (2015) A novel compound against oncogenic Aurora kinase A overcomes imatinib resistance in chronic myeloid leukemia cells, *International journal of oncology 46*, 2488-2496.
37. Aliagas-Martin, I., Burdick, D., Corson, L., Dotson, J., Drummond, J., Fields, C., Huang, O. W., Hunsaker, T., Kleinheinz, T., Krueger, E., Liang, J., Moffat, J., Phillips, G., Pulk, R., Rawson, T. E., Ultsch, M., Walker, L., Wiesmann, C., Zhang, B., Zhu, B.-Y., and Cochran, A. G. (2009) A class of 2,4-bisanilinopyrimidine Aurora A inhibitors with unusually high selectivity against Aurora B, *J. Med. Chem. 52*, 3300-3307.
38. Burgess, S. G., and Bayliss, R. (2015) The structure of C290A:C393A Aurora A provides structural insights into kinase regulation, *Acta Crystallogr F Struct Biol Commun 71*, 315-319.
39. Carry, J.-C., Clerc, F., Minoux, H., Schio, L., Mauger, J., Nair, A., Parmantier, E., Le Moigne, R., Delorme, C., Nicolas, J.-P., Krick, A., Abécassis, P.-Y., Crocq-Stuerga, V., Pouzieux, S., Delarbre, L., Maignan, S., Bertrand, T., Bjergarde, K., Ma, N., Lachaud, S., Guizani, H., Lebel, R., Doerflinger, G., Monget, S., Perron, S., Gasse, F., Angouillant-Boniface, O., Filoche-Rommé, B., Murer, M., Gontier, S., Prévost, C., Monteiro, M.-L., and Combeau, C. (2015) SAR156497, an exquisitely selective inhibitor of aurora kinases, *J. Med. Chem. 58*, 362-375.
40. Gustafson, W. C., Meyerowitz, J. G., Nekritz, E. A., Chen, J., Benes, C., Charron, E., Simonds, E. F., Seeger, R., Matthay, K. K., Hertz, N. T., Eilers, M., Shokat, K. M., and Weiss, W. A. (2014) Drugging MYCN through an allosteric transition in Aurora kinase A, *Cancer Cell 26*, 414-427.
41. Heron, N. M., Anderson, M., Blowers, D. P., Breed, J., Eden, J. M., Green, S., Hill, G. B., Johnson, T., Jung, F. H., McMiken, H. H. J., Mortlock, A. A., Pannifer, A. D., Pauptit, R. A., Pink, J., Roberts, N. J., and Rowsell, S. (2006) SAR and inhibitor complex structure determination of a novel class of potent and specific Aurora kinase inhibitors, *Bioorg. Med. Chem. Lett. 16*, 1320-1323.
42. Martin, M. P., Zhu, J.-Y., Lawrence, H. R., Pireddu, R., Luo, Y., Alam, R., Ozcan, S., Sebti, S. M., Lawrence, N. J., and Schönbrunn, E. (2012) A novel mechanism by which small molecule inhibitors induce the DFG flip in Aurora A, *ACS Chem. Biol. 7*, 698-706.
43. Sarvagalla, S., and Coumar, M. S. (2015) Structural Biology Insight for the Design of Sub-type Selective Aurora Kinase Inhibitors, *Curr Cancer Drug Targets 15*, 375-393.
44. Peifer, C., and Alessi, D. R. (2008) Small-molecule inhibitors of PDK1, *ChemMedChem 3*, 1810-1838.
45. Raimondi, C., Calleja, V., Ferro, R., Fantin, A., Riley, A. M., Potter, B. V., Brennan, C. H., Maffucci, T., Larijani, B., and Falasca, M. (2016) A Small Molecule Inhibitor of PDK1/PLCγ1 Interaction Blocks Breast and Melanoma Cancer Cell Invasion, *Scientific reports 6*.
46. Taga, M., Hirooka, E., and Ouchi, T. (2009) Essential roles of mTOR/Akt pathway in Aurora-A cell transformation, *Int J Biol Sci 5*, 444-450.
47. Gagliardi, P. A., Di Blasio, L., Puliafito, A., Seano, G., Sessa, R., Chianale, F., Leung, T., Bussolino, F., and Primo, L. (2014) PDK1-mediated activation of MRCKα regulates directional cell migration and lamellipodia retraction, *The Journal of cell biology 206*, 415-434.
48. Xie, Z., Yuan, H., Yin, Y., Zeng, X., Bai, R., and Glazer, R. I. (2006) 3-phosphoinositide-dependent protein kinase-1 (PDK1) promotes invasion and activation of matrix metalloproteinases, *BMC cancer 6*, 1.
49. Gagliardi, P. A., di Blasio, L., Orso, F., Seano, G., Sessa, R., Taverna, D., Bussolino, F., and Primo, L. (2012) 3-phosphoinositide-dependent kinase 1 controls breast tumor growth in a kinase-dependent but Akt-independent manner, *Neoplasia 14*, 719-IN719.
50. Joshi, A. D., Loilome, W., Siu, I.-M., Tyler, B., Gallia, G. L., and Riggins, G. J. (2012) Evaluation of tyrosine kinase inhibitor combinations for glioblastoma therapy, *PloS one 7*, e44372.

51. Cammareri, P., Scopelliti, A., Todaro, M., Eterno, V., Francescangeli, F., Moyer, M. P., Agrusa, A., Dieli, F., Zeuner, A., and Stassi, G. (2010) Aurora-a is essential for the tumorigenic capacity and chemoresistance of colorectal cancer stem cells, *Cancer research 70*, 4655-4665.
52. Qin, L., Tian, Y., Yu, Z., Shi, D., Wang, J., Zhang, C., Peng, R., Chen, X., Liu, C., and Chen, Y. (2016) Targeting PDK1 with dichloroacetophenone to inhibit acute myeloid leukemia (AML) cell growth, *Oncotarget 7*, 1395.
53. Fu, Y., Zhang, Y., Gao, M., Quan, L., Gui, R., and Liu, J. (2016) Alisertib induces apoptosis and autophagy through targeting the AKT/mTOR/AMPK/p38 pathway in leukemic cells, *Molecular medicine reports 14*, 394-398.
54. Panicker, S. P., Raychaudhuri, B., Sharma, P., Tipps, R., Mazumdar, T., Mal, A. K., Palomo, J. M., Vogelbaum, M. A., and Haque, S. J. (2010) p300-and Myc-mediated regulation of glioblastoma multiforme cell differentiation, *Oncotarget 1*, 289-303.
55. Nogueira, L., Ruiz-Ontañon, P., Vazquez-Barquero, A., Moris, F., and Fernandez-Luna, J. L. (2011) The NFκB pathway: a therapeutic target in glioblastoma, *Oncotarget 2*, 646-653.
56. Sun, C., Chan, F., Briassouli, P., and Linardopoulos, S. (2007) Aurora kinase inhibition downregulates NF-κB and sensitises tumour cells to chemotherapeutic agents, *Biochemical and biophysical research communications 352*, 220-225.
57. Pahl, H. L. (1999) Activators and target genes of Rel/NF-κB transcription factors, *Oncogene 18*.
58. (2014) V.S.d. Glide, LLC, New York.
59. (2009) V.S. Maestro, LLC, New York.
60. Nagashima, K., Shumway, S. D., Sathyanarayanan, S., Chen, A. H., Dolinski, B., Xu, Y., Keilhack, H., Nguyen, T., Wiznerowicz, M., Li, L., Lutterbach, B. A., Chi, A., Paweletz, C., Allison, T., Yan, Y., Munshi, S. K., Klippel, A., Kraus, M., Bobkova, E. V., Deshmukh, S., Xu, Z., Mueller, U., Szewczak, A. A., Pan, B.-S., Richon, V., Pollock, R., Blume-Jensen, P., Northrup, A., and Andersen, J. N. (2011) Genetic and pharmacological inhibition of PDK1 in cancer cells: characterization of a selective allosteric kinase inhibitor, *J. Biol. Chem. 286*, 6433-6448.
61. Pettersen, E. F., Goddard, T. D., Huang, C. C., Couch, G. S., Greenblatt, D. M., Meng, E. C., and Ferrin, T. E. (2004) UCSF Chimera--a visualization system for exploratory research and analysis, *J Comput Chem 25*, 1605-1612.
62. Hu, Y., and Smyth, G. K. (2009) ELDA: extreme limiting dilution analysis for comparing depleted and enriched populations in stem cell and other assays, *Journal of immunological methods 347*, 70-78.
63. Boyum, A. (1968) Isolation of mononuclear cells and granulocytes from human peripheral blood, *Scand j clin lab invest 21*, 77-89.
64. Costa, B., Bendinelli, S., Gabelloni, P., Da Pozzo, E., Daniele, S., Scatena, F., Vanacore, R., Campiglia, P., Bertamino, A., and Gomez-Monterrey, I. (2013) Human glioblastoma multiforme: p53 reactivation by a novel MDM2 inhibitor, *PloS one 8*, e72281.
65. Daniele, S., Lecca, D., Trincavelli, M. L., Ciampi, O., Abbracchio, M. P., and Martini, C. (2010) Regulation of PC12 cell survival and differentiation by the new P2Y-like receptor GPR17, *Cellular signalling 22*, 697-706.
66. Daniele, S., Giacomelli, C., Zappelli, E., Granchi, C., Trincavelli, M. L., Minutolo, F., and Martini, C. (2015) Lactate dehydrogenase-A inhibition induces human glioblastoma multiforme stem cell differentiation and death, *Scientific reports 5*.
67. Daniele, S., Taliani, S., Da Pozzo, E., Giacomelli, C., Costa, B., Trincavelli, M. L., Rossi, L., La Pietra, V., Barresi, E., and Carotenuto, A. (2014) Apoptosis therapy in cancer: the first single-molecule co-activating p53 and the translocator protein in glioblastoma, *Scientific reports 4*.
68. Daniele, S., Zappelli, E., and Martini, C. (2015) Trazodone regulates neurotrophic/growth factors, mitogen-activated protein kinases and lactate release in human primary astrocytes, *Journal of neuroinflammation 12*, 1.
69. Daniele, S., Da Pozzo, E., Zappelli, E., and Martini, C. (2015) Trazodone treatment protects neuronal-like cells from inflammatory insult by inhibiting NF-κB, p38 and JNK, *Cellular signalling 27*, 1609-1629.

70. Fernando, P., Brunette, S., and Megeney, L. A. (2005) Neural stem cell differentiation is dependent upon endogenous caspase 3 activity, *The FASEB journal 19*, 1671-1673.

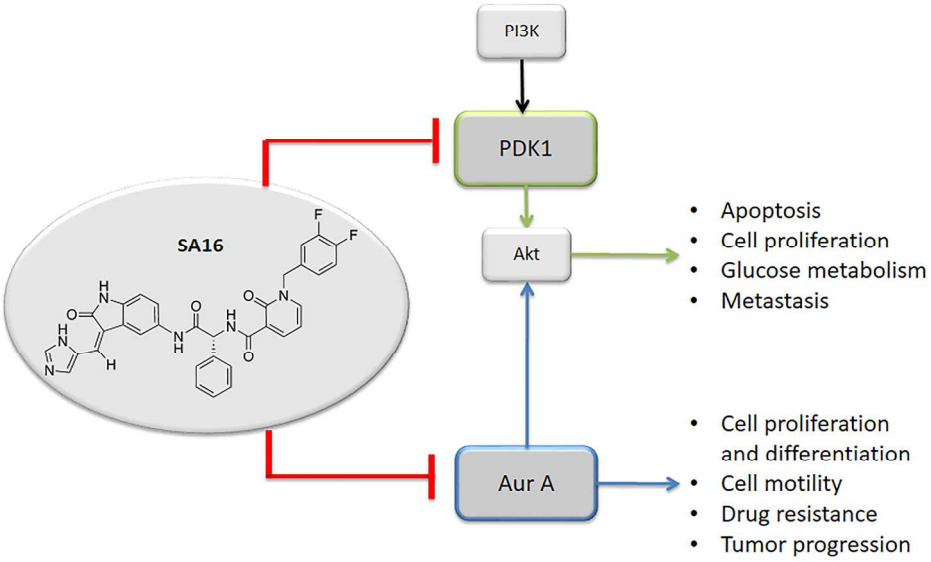

Graphical Table of contents

254x190mm (300 x 300 DPI)